# Intermolecular Interactions of Noble-Gas-Containing Species

Antti Lignell

University of Helsinki
Faculty of Science
Department of Chemistry

Laboratory of Physical Chemistry
P. O. Box 55 (A. I. Virtasen aukio 1)
FIN-00014 University of Helsinki
Finland

**ACADEMIC DISSERTATION**

To be presented, with the permission of the Faculty of Science of the University of Helsinki, for public criticism in the Main lecture hall A110 of the Department of Chemistry (A. I. Virtasen aukio 1) on August 20th 2008, at 12 o'clock noon.

Helsinki 2008

Supervisors

Professor Markku Räsänen and
Docent Leonid Khriachtchev
Laboratory of Physical Chemistry
Department of Chemistry
University of Helsinki


Reviewers

Professor Helge Willner
Fachbereich Chemie
Bergische Universität Wuppertal
Germany

and

Professor Tapani Pakkanen
Department of Chemistry
University of Joensuu
Finland


Opponent

Professor Vladimir Feldman
Department of Chemistry
Moscow State University
Russia

# Acknowledgements

I would like to express my gratitude to our group leader and my supervisor Professor Markku Räsänen. He gave me an excellent opportunity to start my scientific career as a summer trainee after finishing my second year studies at our University and has believed in me and given me his continuous support ever since. My second supervisor, Dr. Leonid Khriachtchev is greatly appreciated for sharing his excellent skills to find and solve scientific problems and redirecting my "famous imagination" to scientifically more relevant directions. I thank Dr. Mika Pettersson for sharing his enthusiasm and courage to explore new scientific phenomena. Professor Jan Lundell is acknowledged for introducing the fascinating field of computational chemistry to me.

Dr. Raimo Timonen, Dr. Esa Isoniemi, Dr. Markus Metsälä, and Mr. Markku Rasilainen are thanked for technical assistance with experimental setup and computers. Professor Benny Gerber, Professor Elena Savchenko, Professor Vladimir Feldman, Professor Alexander Nemukhin, Professor Pekka Pyykkö, Professor Jonas Juselius, Professor Xavier Michaut, Dr. Anastasia Bochenkova, Dr. Juha Vaara, Dr. Pekka Manninen, and Dr. Michal Straka are thanked for useful discussions. I am grateful to Dr. Joseph Guss for correcting the language of this thesis.

Head of our laboratory, Professor Lauri Halonen, and all other present and former members of our laboratory are thanked for their scientific and non-scientific discussions and making us a very warm atmosphere to work. Especially I would like to thank my colleagues Mrs. Hanna Tanskanen and Dr. Aleksandra Domanskaya for sharing office with me and making many of my days brighter.

The Academy of Finland (CoE project Computational Molecular Science), Finnish Ministry of Education (Laskemo Graduate School), University of Helsinki, Association of Finnish Chemical Societies, Magnus Ehrnrooth Foundation, Alfred Kordelin Foundation, and The Nordic Network for Chemical Kinetics are thanked for financial support during this research. CSC – the Finnish IT Center for Science is thanked for providing excellent supercomputing facilities.

I would like to thank my close friends Tusse, Nieminen, Matti, Timuri, Moguli, Viki, Matula, Tiina, Hannu, Maria, and all the others who are not mentioned here by name, for widening my perspective towards life outside the laboratory. Especially I would like to thank my "second father" Kari Tuomainen for sharing his great experience of life with me. I have tried to adapt at least part of this knowledge.

I thank my loving parents Lilli and Simo for encouraging and supporting me to find my own path of life. I dearly thank my ex-partner Anski for sharing a big part of my life, without her this thesis would not have been possible to do. Finally I thank my wife (and colleague) Hanna and the kids Ilka, Meri-Xenia, and "pikku-D" for sharing their love and understanding during this project and making my life lively.


Antti Lignell,
Helsinki, April 2008

# Contents

# 1. List of original publications

This thesis is based on the following publications:

I  Antti Lignell, Leonid Khriachtchev, Mika Pettersson, and Markku Räsänen, *Large blueshift of the H-Kr stretching frequency of HKrCl upon complexation with $N_2$*
J. Chem. Phys. **117**, 961 (2002).

II  Antti Lignell, Leonid Khriachtchev, Mika Pettersson, and Markku Räsänen, *Interaction of rare-gas-containing molecules with nitrogen: Matrix-isolation and ab initio study of HArF⋯$N_2$, HKrF⋯$N_2$, and HKrCl⋯$N_2$ complexes*
J. Chem. Phys. **118**, 11120 (2003).

III  Antti Lignell, Leonid Khriachtchev, Mika Pettersson, and Markku Räsänen, *A study on stabilization of HHeF molecule upon complexation with Xe atoms*
Chem. Phys. Lett. **390**, 256 (2004).

IV  Leonid Khriachtchev, Antti Lignell, Jonas Juselius, Markku Räsänen, and Elena Savchenko, *Infrared absorption spectrum of matrix-isolated noble-gas hydride molecules: Fingerprints of specific interaction and hindered rotation*
J. Chem. Phys. **122**, 014510 (2005).

V  Leonid Khriachtchev, Antti Lignell, and Markku Räsänen, *Neutralization of solvated protons and formation of noble-gas hydride molecules: Matrix-isolation indications of tunneling mechanisms?*
J. Chem. Phys. **123**, 064507 (2005).

VI  Antti Lignell, Leonid Khriachtchev, Hanna Mustalampi, Toni Nurminen, and Markku Räsänen, *Interaction of bihalogen anions with nitrogen: Matrix-isolation study and first principle calculations of the (ClHCl)⁻⋯$N_2$ and (BrHBr)⁻⋯$N_2$ complexes*
Chem. Phys. Lett. **405**, 448 (2005).

VII  Antti Lignell, Leonid Khriachtchev, Hanna Lignell, and Markku Räsänen, *Protons solvated in noble-gas matrices: Interaction with nitrogen*
Phys. Chem. Chem. Phys. **8**, 2457 (2006).

VIII  Antti Lignell, Jan Lundell, Leonid Khriachtchev, and Markku Räsänen, *Experimental and computational study of HXeY⋯HX complexes (X, Y = Cl and Br): An example of exceptionally large complexation effect*
J. Phys. Chem. A **112**, 5486 (2008).

Other publications related to this thesis:

1  Leonid Khriachtchev, Mika Pettersson, Antti Lignell, and Markku Räsänen, *A more stable configuration of HArF in solid argon* J. Am. Chem. Soc. **123**, 8610 (2001).

2  Mika Pettersson, Leonid Khriachtchev, Antti Lignell, Markku Räsänen, Z. Bihary, and R. B. Gerber, *HKrF in solid krypton* J. Chem. Phys. **116**, 2508 (2002).

3  Antti Lignell, Jan Lundell, Mika Pettersson, Leonid Khriachtchev, and Markku Räsänen, *Kr-Cl stretching vibration of HKrCl: Matrix-isolation and anharmonic ab initio study* Low Temp. Phys. **29**, 844 (2003), [originally in Fizika Nizkikh Temperatur **29**, 1109 (2003)].

4  Leonid Khriachtchev, Antti Lignell, and Markku Räsänen, *Formation of HArF in solid Ar revisited: Are mobile vacancies involved in the matrix-site conversion at 30 K?* J. Chem. Phys. **120**, 3353 (2004).

5  Jan Lundell, Sławomir Berski, Antti Lignell, and Zdzisław Latajka, *Quantum chemical study of the hydrogen bonded HXeOH-$H_2O$ complex* J. Mol. Struct. **790**, 31 (2006).

6  Leonid Khriachtchev, Antti Lignell, Hanna Tanskanen, Jan Lundell, Harri Kiljunen, and Markku Räsänen, *Insertion of noble gas atoms into cyanoacetylene: An ab initio and matrix isolation study* J. Phys. Chem. A **110**, 11876 (2006).

7  Antti Lignell, Leonid Khriachtchev, Jan Lundell, Hanna Tanskanen, and Markku Räsänen, *On theoretical predictions of noble-gas hydrides* J. Chem. Phys. **125**, 184514 (2006).

8  Hanna Tanskanen, Susanna Johansson, Antti Lignell, Leonid Khriachtchev, and Markku Räsänen, *Matrix-isolation and ab initio study of the HXeCCH···$CO_2$ complex* J. Chem. Phys. **127**, 154313 (2007).

9  Hanna Tanskanen, Leonid Khriachtchev, Antti Lignell, Markku Räsänen, Susanna Johansson, Ivan Khyzhniy, and Elena Savchenko, *Formation of noble-gas hydrides and decay of solvated protons revisited: Diffusion-controlled reactions and hydrogen atom losses in solid noble gases* Phys. Chem. Chem. Phys. **10**, 692 (2008).

10      Anastasia V. Bochenkova, Leonid Khriachtchev, Antti Lignell, Markku Räsänen, Hanna Lignell, Alexander A. Granovsky, and Alexander V. Nemukhin, *Hindered rotation of HArF in solid argon: Infrared spectroscopy and a theoretical model*
Phys. Rev. B **77**, 094301 (2008).

11      Antti Lignell and Leonid Khriachtchev, *Intermolecular interactions involving noble-gas hydrides: Where the blue shift of vibrational frequency is a normal effect*
J. Mol. Struct. *Accepted for publication* (2008).

# 2. Abbreviations

| | |
|---|---|
| BSSE | basis set superposition error |
| CP | counterpoise correction |
| DIIS | direct inversion of iterative subspace |
| DIM | diatomics-in-molecules |
| DNA | deoxyribonucleic acid |
| E(bond) | bonding energy |
| E(int) | interaction energy |
| ECP | effective core potential |
| FTIR | Fourier transform infrared spectrometer |
| H-bond | hydrogen bond |
| HF | Hartree-Fock |
| IR | infra red |
| MCT | mercury cadmium telluride |
| MP2 | Møller-Plesset second order perturbation theory |
| Nd:YAG | neodymium-doped yttrium aluminum garnet |
| Ng | noble gas |
| NPA | natural population analysis |
| OPO | optical parametric oscillator |
| QC | quadratically convergent |
| QM/MM | quantum mechanics/molecular mechanics |
| S/M | sample/matrix |
| SCF | self-consistent field |
| TS | transition state |
| UV | ultra violet |
| ZPE | zero-point energy |

# 3. Introduction

The importance of intermolecular interactions to chemistry, physics, and biology is difficult to overestimate. Without intermolecular forces, condensed phase matter could not form. The simplest way to categorize different types of intermolecular interactions is to describe them using van der Waals and hydrogen bonded (H-bonded) interactions. The van der Waals complex is a general description of an intermolecular interaction including all of the intermolecular force components and the H-bond is a special case of van der Waals interactions. In the H-bond, the intermolecular interaction appears between a positively charged hydrogen atom and electronegative fragments and it originates from strong electrostatic interactions.[1,2] The intermolecular interactions in H-bonds are typically stronger than those in van der Waals complexes but weaker than those in chemical bonds. H-bonding is important when considering the properties of condensed phase water and in many biological systems including the structure of DNA and proteins.[3]

Vibrational spectroscopy is a useful tool for studying complexes and the solvation of molecules.[4,5] Vibrational frequency shift has been used to characterize complex formation. In an H-bonded system A···H-X (A and X are acceptor and donor species, respectively), the vibrational frequency of the H-X stretching vibration usually decreases from its value in free H-X (red-shift). This frequency shift has been used as evidence for H-bond formation and the magnitude of the shift has been used as an indicator of the H-bonding strength.[6] In contrast to this "normal" behavior are the blue-shifting H-bonds, in which the H-X vibrational frequency increases upon complex formation. In the last decade, there has been active discussion regarding these blue-shifting H-bonds.[7-11]

Possibly the first reports of blue-shifting H-bonds were made in the late 1950's by Pinchas, who demonstrated an intramolecular H-bond formation in various aldehydes.[12-15] Later, this unusual effect – especially in systems that contain halogen substitutes – was described in a number of articles. As an example of these studies, the complexes of trifluoromethane (fluoroform) and trichloromethane (chloroform) with various molecules (e.g. triformylmethane and fluorobenzene) show blue shifts of the C-H stretching mode in the complexed trihalogenomethane molecules.[16-19] The physical origins of the blue-shifting H-bonds have been studied;[20-25] however, efforts to explain this phenomenon with a universal model are ongoing.

Noble-gases have been considered "inert" due to their limited reactivity with other elements. In the early 1930's, Pauling predicted the stable noble-gas compounds $XeF_6$ and $KrF_6$.[26] It was not until three decades later Neil Bartlett synthesized the first noble-gas compound, $XePtF_6$, in 1962.[27] Later, noble-gas chemistry was expanded to include compounds of krypton and radon.[28,29] A "renaissance" of noble-gas chemistry began in 1995 with the discovery of noble-gas hydride molecules at the University of Helsinki.[30-32] The first hydrides were HXeCl, HXeBr, HXeI, HKrCl, and HXeH. These molecules have the general formula of HNgY, where H is a hydrogen atom, Ng is a noble-gas atom (Ar, Kr, or Xe), and Y is an electronegative fragment. At present, this class of molecules comprises 23 members including both inorganic and organic compounds.[33-36] The first and only argon-containing neutral chemical compound HArF was synthesized in 2000 and its properties have since been investigated in a number of studies.[37-42] Much computational

works on noble-gas hydrides has also taken place, including studies of their life-times and solid state dynamics.[43-50] A helium-containing chemical compound, HHeF, was predicted computationally, but its lifetime has been predicted to be severely limited by hydrogen tunneling.[51-55] Helium and neon are the only elements in the periodic table that do not form neutral, ground state molecules.

The HNgY molecules are chemically bound systems. They have a strong $(HNg)^+Y^-$ ion-pair character, which leads to a large dipole moment at the equilibrium geometry.[33-36] The H-Ng bond is mainly covalent and the Ng-Y bond is mainly ionic with some covalent contribution.[56] The intense absorption of the H-Ng stretching modes makes these molecules easy to detect with infra red (IR) spectroscopy. Most of the experiments on HNgY molecules were performed in low-temperature noble-gas matrices, but recently some HXeY species have been found in gas-phase xenon clusters.[57-60] The HNgY molecules have very strong interactions with their surroundings as demonstrated by the large splitting of their vibrational bands between different solid state configurations (matrix sites).[38,61,62] The formation mechanism of these molecules has been discussed and these molecules most probably form from the neutral H + Ng + Y fragments upon thermal hydrogen diffusion in matrices.[33-36] An intriguing question is weather or not HNgY can form as isolated molecules in the gas phase or in the crystalline form. Computations have predicted the stable crystal formation of the HXeH and HXeCCH molecules.[63,64]

A noble-gas matrix is a useful medium in which to study unstable and reactive species including ions.[4,5] A solvated proton forms a centrosymmetric $NgHNg^+$ (Ng = Ar, Kr, and Xe) structure in a noble-gas matrix and this is probably the simplest example of a solvated proton.[65-73] Interestingly, the hypothetical $NeHNe^+$ cation is isoelectronic with the water-solvated proton $H_5O_2^+$ (Zundel-ion).[74-76] The $NgHNg^+$ species can be trapped by depositing a mixture of hydrogen-containing precursor molecules and noble gas through a discharge onto a cold substrate, or by photolyzing precursor molecules in noble-gas solids.[65,69] The infrared absorptions of these ions were first characterized in noble-gas matrices in the early 1970's but their exact molecular structure remained uncertain at that time.[65,68] It was later observed, that in solid noble gases a proton is solvated to form a linear triatomic $NgHNg^+$ structure.[69,70] Due to strong anharmonicity, these ions exhibit a very strong coupling between the symmetric ($\nu_1$) and antisymmetric ($\nu_3$) stretching vibrations, leading to the characteristic $\nu_3+n\nu_1$ combination bands. The $NgHNg^+$ absorptions decay at low temperatures and the mechanism of this decay has been a puzzle for many years.[65-67] This cation decay has a noticeable H/D isotope effect. It has been suggested that room-temperature black body radiation and tunneling-assisted proton diffusion could explain the dark decay of the $NgHNg^+$ bands.[77-78]

In addition to the $NgHNg^+$ cations, the isoelectronic $YHY^-$ (Y = halogen atom or pseudohalogen fragment) anions have been studied with the matrix-isolation technique.[79-84] These species have been known to exist in alkali metal salts $(YHY)^-M^+$ (M = alkali metal e.g. K or Na) for more than 80 years.[85] Hydrated HF forms the $FHF^-$ structure in aqueous solutions, and these ions participate in several important chemical processes.[86] $YHY^-$ anions have a centrosymmetric structure and they show vibrational combination bands similar to those of the $NgHNg^+$ cations.[69,70] It was suggested that both $YHY^-$ and $NgHNg^+$ ions can be described in terms of a strong H-bond between the

hydrogen and halogen atoms.[69,84] In our opinion, these species are more likely to be true chemically bound systems due to their fully delocalized electron density, equal bond lengths, and large bond energies, typical for normal chemical bonds.[87-89]

In this thesis, studies of the intermolecular interactions of HNgY molecules and centrosymmetric ions with various species are presented. The HNgY complexes show unusual spectral features, e.g. large blue-shifts of the H-Ng stretching vibration upon complexation. It is suggested that the blue-shift is a "normal" effect for these molecules, and that originates from the enhanced $(HNg)^+Y^-$ ion-pair character upon complexation. It is also found that the HNgY molecules are energetically stabilized in the complexed form, and this effect is computationally demonstrated for the HHeF molecule.[51-55] The $NgHNg^+$ and $YHY^-$ ions also show blue-shifts in their asymmetric stretching vibration upon complexation with nitrogen.

Additionally, the matrix site structure and hindered rotation (libration) of the HNgY molecules were studied. The librational motion is a much-discussed solid state phenomenon,[90-95] and the HNgY molecules embedded in noble-gas matrices are good model systems to study this effect. The formation mechanisms of the HNgY molecules and the decay mechanism of $NgHNg^+$ cations are discussed. A new electron tunneling model for the decay of $NgHNg^+$ absorptions in noble-gas matrices is proposed. Studies of the $NgHNg^+\cdots N_2$ complexes support this electron tunneling mechanism.

# 4. Methods

## 4.1. Experimental

Standard matrix-isolation techniques are used in the experiments (see Fig. 1).[4,5] The sample (S) and matrix (M) gases are mixed in a glass bulb at typical S/M ratios of 1:(2000-300). The gas mixtures are deposited onto a cold (8-60 K) CsI substrate in a closed-cycle helium cryostat (APD, DE 202A) and the typical matrix thickness was ~100 μm. A needle valve was used to control the gas flow rate. In the experiments with HF, the matrix gas flushed a HF-pyridine polymer (Fluka) at room temperature. In some experiments, impurity water was removed from the sample gas flow by depositing it over drops of sulfuric acid. Deuteration of HF was achieved by passing the sample gases through deuterated sulfuric acid.
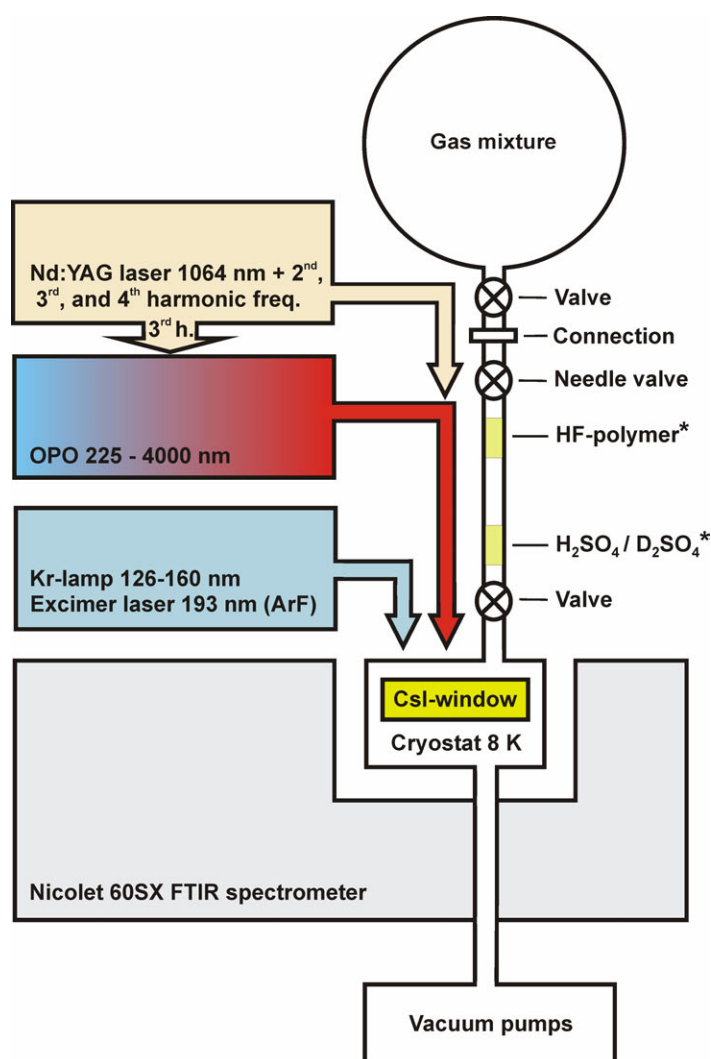


**Figure 1.** *Matrix isolation setup. HF-polymer and sulfuric acid (\*) were used only in some experiments.*

14

The IR absorption spectra were typically recorded at 8 K with a Nicolet 60SX FTIR spectrometer with resolutions of 1 and 0.25 cm$^{-1}$ by co-adding up to 1000 interferograms. The spectra were measured in the 400 to 4000 cm$^{-1}$ range using a liquid-nitrogen-cooled MCT-A detector and Ge-KBr beam splitter. The matrices were photolyzed through a MgF window at 8 K by an ArF excimer laser (MPB, MSX-250) emitting at 193 nm (pulse energy ≤15 mJ cm$^{-2}$), a krypton continuum lamp (Opthos) emitting in the 127-160 nm spectral range (microwave power ~40 W), or by an optical parametric oscillator tunable from 225 nm to 4 µm (Continuum, 10 Hz, ~10 mJ cm$^{-2}$). The matrices were annealed at up to 70 K. In some experiments, the spectra were measured at elevated temperatures.

## 4.2. Theory and computations

### 4.2.1. Electronic structure calculations

The minimum energy structures of the intra- and intermolecular potential energy surfaces were obtained with Møller-Plesset second order perturbation theory (MP2) by including all of the electrons explicitly in the correlation calculation.[96] Preliminary structures of the complexes were first optimized at the Hatree-Fock (HF) level of theory.[97] Quadratically converged (QC) and Pulay's direct inversion of iterative subspace extrapolation (DIIS) procedures were used for the self-consistent field (SCF) calculations.[98,99] The program packages used were Gaussian 98 and 03 (various revisions) and Gamess (various revisions) running on the SGI Origin 2000, the IBM eServer Cluster 1800, and the Sun Fire 25K computers at CSC – Center for Scientific Computing Ltd. (Espoo Finland).[100,101]

The basis sets used were taken from the internal library of the Gaussian packages or downloaded from the EMSL basis set library.[102,103] They were standard basis sets according to the Dunning's and Pople's notation. Dunning's basis sets include correlation consistence valence double- and triple-zeta (aug)-cc-pVXZ (X = D or T) basis sets typically augmented with the diffuse functions.[104,105] The split valence basis set of 6-311++G(2d,2p) was also used.[106-108] For xenon and (in some systems) bromine atoms, the Stuttgart/Dresden (SDD),[109] small-core Stuttgart,[110] and LaJohn effective core potentials (ECPs) were employed.[111] For xenon and bromine atoms, the valence space optimized by Runeberg and Pyykkö, and cc-pVTZ-PP were used, respectively, together with ECPs.[112]

The charge distributions were calculated with Mulliken and natural population analysis (NPA) methods.[113,114] The vibrational frequencies were obtained at the MP2 level using harmonic force fields.

## 4.2.2. Intermolecular interactions

The interaction energies of the complexes were estimated as the difference between the energy of the complex and that of the monomers. The basis set superposition error (BSSE) was minimized by the counterpoise (CP) correction method developed by Boys and Bernardi.[115] The vibrational zero-point energy correction was used in most of the intermolecular energy calculations.

The intermolecular energy component analysis was performed by dividing the energy components into electrostatic, induction, dispersive, and repulsive interactions.[116] The electrostatic interactions can be calculated using the electrostatic interaction energy that takes into account interactions between the static dipole and quadrupole moments:

$$U_{AB} = \frac{\mu_A \mu_B}{4\pi\varepsilon_0 r^3} f_1 + \frac{\mu_A \Theta_B}{4\pi\varepsilon_0 r^4} f_2 - \frac{\mu_B \Theta_A}{4\pi\varepsilon_0 r^4} f_2 + \frac{\Theta_A \Theta_B}{4\pi\varepsilon_0 r^5} f_3$$

$$f_1 = \sin\varphi_A \sin\varphi_B \cos\theta - 2\cos\varphi_A \cos\varphi_B$$

(1)
$$f_2 = \frac{3}{2}\left[\cos\varphi_A \left(3\cos^2\varphi_B - 1\right) - 2\sin\varphi_A \sin\varphi_B \cos\varphi_B \cos\theta\right]$$

$$f_3 = \frac{3}{4}\left[\begin{array}{l}1 - 5\cos^2\varphi_A - 5\cos^2\varphi_B - 15\cos^2\varphi_A \cos^2\varphi_B \\ +2\left(4\cos\varphi_A \cos\varphi_B - \sin\varphi_A \sin\varphi_B \cos\theta\right)^2\end{array}\right]$$

where $\mu_A$ and $\Theta_B$ are the dipole moment of molecule A and the quadrupole moment of molecule B. $\varphi$'s are the angles, $\theta$ is the torsion angle between the dipoles of the molecules and $r$ is the distance between the centers of the dipoles of the complex partners. See Reference [116] for a description of the angles.

The induction interaction can be determined by taking into account the dipole-induced dipole term:

(2)
$$U_{AB} = -\alpha\mu^2 \frac{3\cos^2\varphi + 1}{2\left(4\pi\varepsilon_0\right)^2 r^6}$$

where $\alpha$ is the polarizability of the polarizing complex partner and $\varphi$ is the angle between the dipoles.

The dispersion and repulsion interactions can be calculated using the anisotropic Lennard-Jones (6-12) potential function:[117,118]

$$U_{AB} = \varepsilon(\varphi)\left\{\left[\frac{r(\varphi)}{r}\right]^{12} - 2\left[\frac{r(\varphi)}{r}\right]^{6}\right\}$$

(3)
$$\varepsilon(\varphi) = \varepsilon\left[1 + aP_2(\cos\varphi)\right]$$

$$r(\varphi) = \varepsilon\left[1 + bP_2(\cos\varphi)\right]$$

$$P_2(x) = \frac{3}{2}x^2 - \frac{1}{2}$$

A more advanced approach to estimate the intermolecular energy components was accomplished with the Morokuma-Kitaura scheme using the Gamess program package.[101,119,120] The HNgY···N$_2$ complexes were analyzed at the HF level of theory with the aug-cc-pVDZ basis set. The geometry optimizations were performed with the MP2/aug-cc-pVDZ level of theory. At this level, the interactions can be divided into electrostatic, polarization, charge-transfer, and exchange-repulsion energy components. The dispersive energy components were estimated as an interaction energy difference ($\Delta E$) of the same complex geometry at the MP2 and HF levels of theory:

(4)
$$\Delta E_{disp} = \Delta E(MP2) - \Delta E(HF)$$

This approach has been demonstrated to give reasonable values for dispersive energy components.[121,122] For the HNgY···HX complexes, the interaction energy component analysis was expanded to the second-order perturbation theory (MP2) with the variation-perturbation scheme. A more complete description of this method is presented in Reference [123]. The basis sets used for HNgY···HX energy component calculations were aug-cc-pVTZ (H atom), cc-pVTZ (Cl atom), and cc-pVTZ-PP (Xe and Br atoms).

# 5. HNgY complexes

The first prediction of noble-gas hydride complexes was made by Lundell *et al.* in a computational study of the H-bonded HXeH···H$_2$O complex.[124,125] Later, experimental and computational studies of HKrCl···N$_2$ and HXeOH···(H$_2$O)$_n$ ($n$ = 1,2) were published.[(Article I),126] This research led to many more computational studies of new HNgY complexes.[63,64,127-157] Of particular note is the work of McDowell, who made computational studies of the HNgY complexes with N$_2$, CO, CO$_2$, H$_2$C$_2$, and hydrogen halides. At present, experimental observations of the following HNgY complexes have been reported: HArF···N$_2$, HKrF···N$_2$, HKrCl···N$_2$, HXeBr···HBr, HXeBr···HCl, HXeCl···HCl, HXeCCH···CO$_2$, and HXeOH···(H$_2$O)$_n$ ($n$ = 1,2).[(Articles I,II,VIII),126,158]

## 5.1. Computational results

### 5.1.1. Structure and vibrational properties

Three groups of complexes are studied here: (1) HNgY···N$_2$, (2) HNgY···HX, and (3) HNgY···Ng. The minimum energy structures of these HNgY complexes are presented in Figures 2 and 3. The structural parameters and partial charges are shown in Table 1.
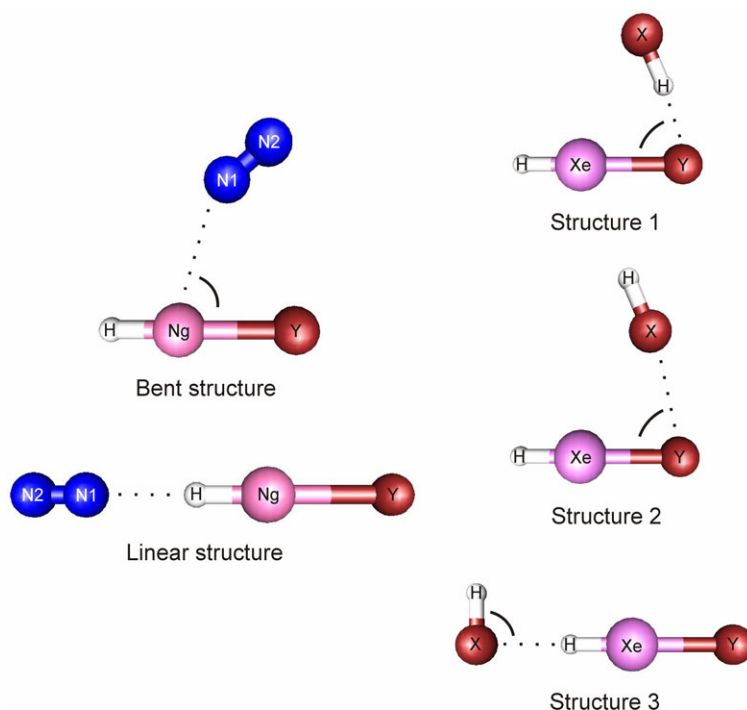


**Figure 2.** *Computational minimum-energy structures of the HArF···N$_2$, HKrF···N$_2$, HKrCl···N$_2$, and HXeY···HX (X,Y = Cl and Br) complexes. The structural parameters are presented in Table 1.*

**Table 1.** *Bond lengths r (in Å), angles (in degrees), and NPA partial charges of HNgY complexes. Structural parameters refer to Fig. 2. The computational level is MP2/6-311++G(2d,2p) for HNgY···N₂ complexes and MP2/aug-cc-pVTZ (H atom), cc-pVTZ (Cl atom), cc-pVTZ-PP (Xe and Br atoms) for HXeY···HX complexes.*

| | r (H-Ng) | r (Ng-Y) | r (interm.) | r (N-N/H-X) | angle | q (H) | q (Ng) | q (Y) |
|---|---|---|---|---|---|---|---|---|
| **HArF···N₂** | | | | | | | | |
| monomer | 1.326 | 1.996 | – | 1.113 | – | 0.225 | 0.536 | −0.761 |
| bent | 1.322 | 2.004 | 3.252 | 1.112 | 66.1 | 0.233 | 0.539 | −0.768 |
| linear | 1.314 | 2.027 | 2.149 | 1.112 | 180.0 | 0.264 | 0.526 | −0.807 |
| **HKrF···N₂** | | | | | | | | |
| monomer | 1.467 | 2.075 | – | 1.113 | – | 0.087 | 0.649 | −0.736 |
| bent | 1.465 | 2.081 | 3.406 | 1.112 | 62.0 | 0.117 | 0.652 | −0.767 |
| linear | 1.461 | 2.090 | 2.413 | 1.113 | 180.0 | 0.132 | 0.642 | −0.781 |
| **HKrCl···N₂** | | | | | | | | |
| monomer | 1.500 | 2.551 | – | 1.113 | – | | | |
| bent | 1.495 | 2.558 | 3.387 | 1.113 | 72.0 | 0.123 | 0.562 | −0.682 |
| linear | 1.465 | 2.537 | 2.195 | 1.110 | 178.9 | 0.149 | 0.559 | −0.720 |
| **HXeBr···HBr** | | | | | | | | |
| monomer | 1.688 | 2.744 | – | 1.398 | – | −0.033 | 0.655 | −0.622 |
| structure 1 | 1.661 | 2.970 | 2.200 | 1.436 | 76.2 | −0.016 | 0.679 | −0.589 |
| structure 2 | 1.681 | 2.755 | 3.524 | 1.402 | 75.3 | −0.022 | 0.662 | −0.627 |
| structure 3 | 1.683 | 2.773 | 2.556 | 1.401 | 91.1 | −0.014 | 0.644 | −0.669 |
| **HXeBr···HCl** | | | | | | | | |
| monomer | 1.688 | 2.744 | – | 1.271 | – | −0.033 | 0.655 | −0.622 |
| structure 1 | 1.662 | 2.797 | 2.213 | 1.305 | 76.3 | 0.015 | 0.679 | −0.605 |
| structure 2 | 1.685 | 2.748 | 3.606 | 1.273 | 72.0 | −0.029 | 0.659 | −0.625 |
| structure 3 | 1.680 | 2.766 | 2.573 | 1.273 | 99.3 | −0.009 | 0.649 | −0.662 |
| **HXeCl···HBr** | | | | | | | | |
| monomer | 1.673 | 2.593 | – | 1.398 | – | −0.028 | 0.694 | −0.666 |
| structure 1 | 1.648 | 2.656 | 2.049 | 1.439 | 80.3 | 0.024 | 0.714 | −0.634 |
| structure 2 | 1.667 | 2.605 | 3.399 | 1.402 | 79.5 | −0.018 | 0.700 | −0.671 |
| structure 3 | 1.669 | 2.621 | 2.569 | 1.401 | 92.6 | −0.011 | 0.679 | −0.704 |
| **HXeCl···HCl** | | | | | | | | |
| monomer | 1.673 | 2.593 | – | 1.271 | – | −0.028 | 0.694 | −0.666 |
| structure 1 | 1.648 | 2.655 | 2.059 | 1.308 | 80.3 | 0.023 | 0.714 | −0.647 |
| structure 2 | 1.670 | 2.598 | 3.503 | 1.272 | 75.8 | −0.025 | 0.698 | −0.669 |
| structure 3 | 1.667 | 2.615 | 2.573 | 1.273 | 99.6 | −0.007 | 0.685 | −0.699 |

For the $N_2$ complexes of HArF, HKrF, and HKrCl, two stable structures (linear and bent) are found. The HCl and HBr complexes of HXeCl and HXeBr show three minimum energy structures, here labeled structures 1-3. The linear structure of the $N_2 \cdots$HNgY and structures 1 and 3 of the HXeY$\cdots$HX complexes are H-bonded. The bent structures of HNgY$\cdots N_2$ and structure 2 of HXeY$\cdots$HX are van der Waals complexes. In addition to 1:1 complexes, we calculated the HXeBr$\cdots$(HBr)$_2$ trimer (see Fig. 3). Complexation shortens the H-Ng bond and elongates the Ng-Y bond of HNgY molecules.

Upon complexation, the internal $(HNg)^+Y^-$ ion-pair character of the HNgY molecules increases in many cases, resulting in stabilization of the H-Ng bond. The characteristics of the H-Ng entity in these molecules approaches those of the free $HNg^+$ cation with a shorter bond length, higher H-Ng vibrational frequency, and lower IR absorption intensity.[159,160] The computational charges (NPA) and the H-Ng vibrational frequencies are collected in Table 1.

The HXeBr$\cdots$Xe structures are shown in Figure 3 and the frequency shifts upon complexation are presented in Table 2. The complexes show three energy minima and two of these structures (1 and 3) are quite similar to the linear and bent structures of the HNgY$\cdots N_2$ complexes. Complexation induced H-Xe vibrational shifts are quite small ($<10$ cm$^{-1}$) and interestingly, structure 2 shows a red shift of 7.6 cm$^{-1}$, instead of the typical blue shift in HNgY complexes.
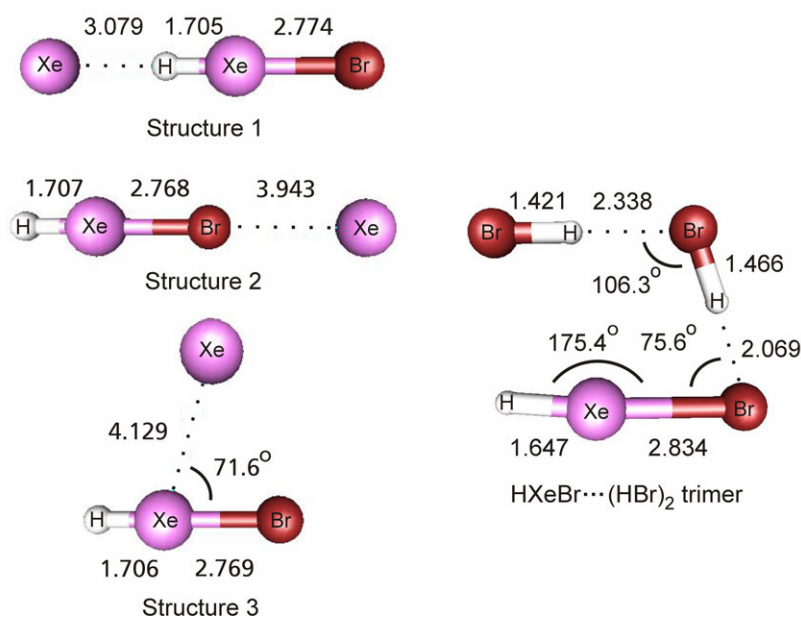


**Figure 3.** *Computational structures of HXeBr$\cdots$Xe complexes MP2/6-311++G(2d,2p),LJ18 (Xe atom) and HXeBr$\cdots$(HBr)$_2$ trimer at MP2/aug-cc-pVTZ (H atom), cc-pVTZ (Cl atom), cc-pVTZ-PP (Xe and Br atoms) levels of theory. Bond lengths are in Å.*

**Table 2.** *Computational monomer-to-complex shifts (in cm$^{-1}$) of the H-Ng stretching vibrations of HNgY complexes. The IR absorption intensities are presented in parentheses (in km mol$^{-1}$). Computational levels are given in Table 1 and in Figure 3.*

|  | HArF···N$_2$ | HKrF···N$_2$ | HKrCl···N$_2$ |
|---|---|---|---|
| monomer | 2148.7 (1150) | 2138.3 (634) | 1828.4 (2412) |
| linear | +155.2 (82) | +64.8 (214) | +145.7 (907) |
| bent | +34.2 (658) | +15.8 (72) | +31.0 (2189) |

|  | HXeBr···HBr[a] | HXeBr···HCl | HXeCl···HBr | HXeCl···HCl | Xe···HXeBr |
|---|---|---|---|---|---|
| monomer | 1818.3 (1734) | 1818.3 (1734) | 1920.1 (1144) | 1920.1 (1144) | 1792.9 (1631) |
| structure 1 | +119.1 (1193) | +122.1 (1201) | +112.4 (764) | +116.7 (733) | +6.5 (1253) |
| structure 2 | +26.5 (1552) | +10.9 (1638) | +23.7 (1013) | +9.9 (1076) | −7.6 (1914) |
| structure 3 | +17.7 (350) | +47.9 (633) | +8.8 (181) | +35.6 (352) | +2.7 (1502) |

[a] monomer-to-complex shift for the tentative HXeBr···(HBr)$_2$ trimer is +251.7 (1884)

## 5.1.2. Energetics

Neutral repulsive and ionic potential energy surfaces contribute to the bonding of the HNgY molecules.[33-36,161] The avoided crossing between these potential energy surfaces makes possible the formation of these molecules from neutral H + Ng + Y fragments.[34] The energy of the identified HNgY is lower than that of the corresponding neutral fragments, and allows for the formation of these molecules from neutral fragments at low temperatures.

Complexation of HNgY molecules lowers the electronic energy by the intermolecular interaction energy [E(int)]. The energy diagram of HNgY complexes is presented in Figure 4. The basis set superposition error (BSSE) and vibrational zero-point energy (ZPE,vib) typically weaken the interaction energy of the complexes. The BSSE corrected interaction energies of the HNgY complexes studied are presented in Table 3.
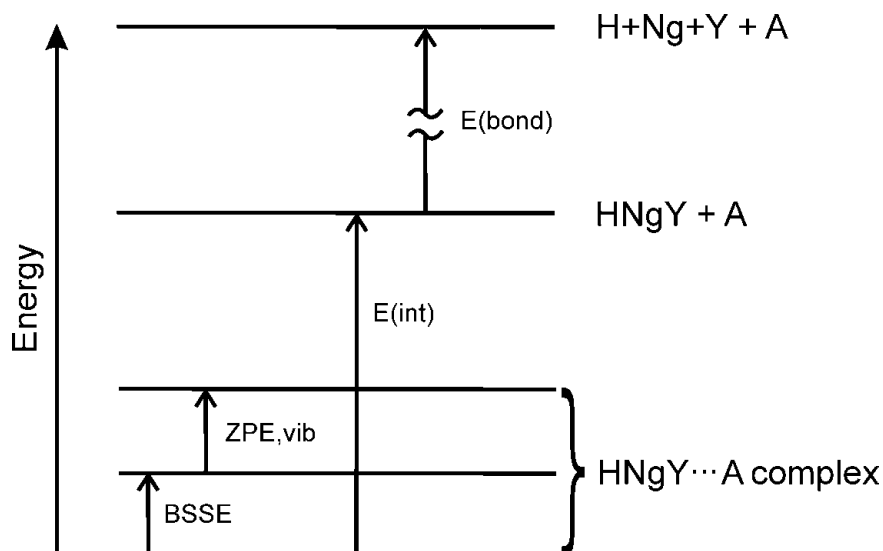
**Figure 4.** *Energy-level diagram of HNgY molecules and their complexes. BSSE and ZPE,vib refer to the basis set superposition error and the vibrational zero-point energy corrections of the interaction energy [E(int)], respectively. E(bond) is the bonding energy of HNgY with respect to the neutral asymptote.*

**Table 3.** *BSSE-corrected interaction energies of the HNgY complexes (in $cm^{-1}$). Computational levels are the same as in Table 1 and Figure 3.*

| | $HArF{\cdots}N_2$ | $HKrF{\cdots}N_2$ | $HKrCl{\cdots}N_2$ |
|---|---|---|---|
| linear | −783 | −394 | −442 |
| bent | −636 | −546 | −613 |

| | $HXeBr{\cdots}HBr$[a] | $HXeBr{\cdots}HCl$ | $HXeCl{\cdots}HBr$ | $HXeCl{\cdots}HCl$ | $Xe{\cdots}HXeBr$ |
|---|---|---|---|---|---|
| structure 1 | −2384 | −2534 | −2638 | −2838 | −261 |
| structure 2 | −792 | −471 | −799 | −488 | −251 |
| structure 3 | −490 | −472 | −501 | −460 | −430 |

[a] interaction energy of $HXeBr{\cdots}(HBr)_2$ trimer is −4580 $cm^{-1}$

The nature of interaction in these complexes was studied with the Morokuma-Kitaura analysis and variation-perturbation scheme.[101,119,120,123] The results of the energy component analyses are collected in Table 4. In many cases, the electrostatic interactions contribute strongly to the total interaction energy. For the bent structure of the $N_2$ complexes and structures 2 and 3 of the HNgY$\cdots$HX complexes, the dispersive interactions compete with the electrostatic forces.

**Table 4.** *Relative contributions of the interaction energy components of the HNgY complexes. The structures refer to Figure 2. The delocalization energy component in the HNgY···HX complexes contains polarization and charge transfer energy contributions.*

|          |                  | HArF···N$_2$ | HKrF···N$_2$ | HKrCl···N$_2$ |
|----------|------------------|--------------|--------------|---------------|
| **linear** | electrostatic   | 36 %         | 39 %         | 37 %          |
|          | polarization     | 30 %         | 18 %         | 22 %          |
|          | charge transfer  | 25 %         | 21 %         | 24 %          |
|          | dispersion       | 9 %          | 21 %         | 17 %          |
| **bent** | electrostatic    | 38 %         | 37 %         | 34 %          |
|          | polarization     | 18 %         | 16 %         | 16 %          |
|          | charge transfer  | 13 %         | 14 %         | 12 %          |
|          | dispersion       | 31 %         | 36 %         | 39 %          |

|              |                | HXeBr···HBr | HXeBr···HCl | HXeCl···HBr | HXeCl···HCl |
|--------------|----------------|-------------|-------------|-------------|-------------|
| **structure 1** | electrostatic | 41 %       | 44 %        | 43 %        | 46 %        |
|              | delocalization | 30 %        | 29 %        | 30 %        | 29 %        |
|              | dispersion     | 29 %        | 27 %        | 27 %        | 26 %        |
| **structure 2** | electrostatic | 43 %       | 38 %        | 44 %        | 38 %        |
|              | delocalization | 15 %        | 13 %        | 15 %        | 13 %        |
|              | dispersion     | 42 %        | 49 %        | 41 %        | 48 %        |
| **structure 3** | electrostatic | 36 %       | 40 %        | 36 %        | 40 %        |
|              | delocalization | 28 %        | 23 %        | 27 %        | 23 %        |
|              | dispersion     | 36 %        | 38 %        | 36 %        | 38 %        |

## 5.2. Experimental results and discussion

Hydrogen halides are among the most studied systems in noble-gas matrices. Their vibrational and rotational properties, photochemistry, and complexes are well known in various hosts.[73,162-168] Our spectra of hydrogen-halide precursors in various matrices are in good agreement with the literature data. Figure 5 represents the HX/N$_2$/Ng (X = F, Cl and Ng = Ar, Kr) matrices with the characteristic HF and HCl related absorption.
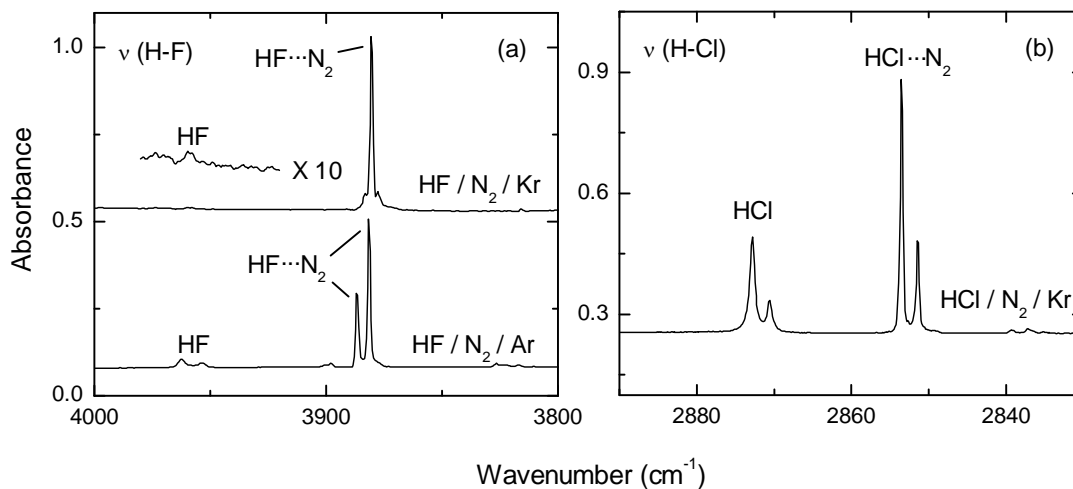
**Figure 5.** *FTIR spectra of HX/N₂/Ng (X = F, Cl and Ng = Ar, Kr) matrices measured at 8 K after deposition.*

### 5.2.1 HNgY⋯N₂ complexes

HF in argon and krypton matrices, and HCl in a krypton matrix were studied. After annealing a photolyzed matrix, the known absorptions of HArF, HKrF, and HKrCl rise in the spectra.[30,38,56,61] In experiments with the $N_2$ dopant, additional absorptions appear close to the HNgY bands after annealing. These absorptions are assigned to HNgY⋯$N_2$ complexes.

The experimental assignment of HNgY⋯$N_2$ complexes is based on the following arguments. The bands assigned to the complexes appear only in experiments with nitrogen doping. Upon annealing, the complex bands rise synchronously with the monomer bands. Also, the photostability of the monomer bands are similar to those of the complex bands. The experimental absorptions of the HNgY⋯$N_2$ complexes are in agreement with the computational predictions. The presence of higher order HNgY⋯$(N_2)_n$ ($n > 1$) complexes was ruled out by experiments with high nitrogen doping.

The IR bands of the HKrCl⋯$N_2$ complexes are presented in Figure 6 and the monomer-to-complex shifts of these absorptions are collected in Table 5. The new absorptions are separated into three groups corresponding to different complex structures. The absorptions were strongest in the H-Kr stretching region, but the complex bands were also observed in the HKrCl bending fundamental region at 541.5 cm$^{-1}$ and in the bending overtone region at 1067.0 cm$^{-1}$.
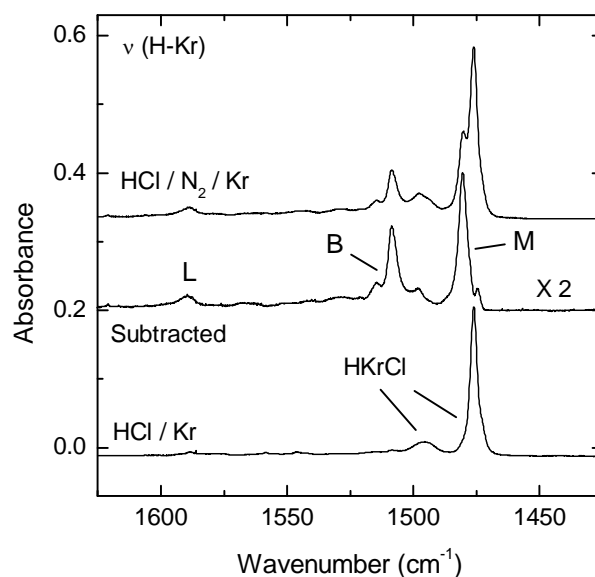
24

**Figure 6.** *FTIR spectra of HKrCl and its $N_2$ complexes. The $N_2$ induced bands are assigned to the linear complex (L), the bend complex (B), and the HKrCl monomer (M) in local matrix surroundings perturbed by $N_2$. The middle trace is a spectrum in which HKrCl bands have been subtracted from the complex bands.*

We assign the bands labeled with L and B to the linear and bent configurations of the HKrCl···$N_2$ complexes. For the linear complex, the exceptionally large blue shift of +112.9 cm$^{-1}$ was in agreement with the computational prediction of +145.7 cm$^{-1}$. The bent complex also shows a large blue shift (+32.4 cm$^{-1}$) in accord with the computational value (+31.0 cm$^{-1}$). The structure marked with an M is probably related to the HKrCl monomer in a perturbed local matrix morphology or a "loose" longer-range interaction with nitrogen.[169,170]

HArF and HKrF molecules appear in several matrix sites with different thermal stability.[38,61] These matrix sites are called thermally stable (S) and unstable (U) structures. Thermally unstable bands appear at lower temperatures and disappear upon annealing at higher temperatures. This behaviour is connected to the relaxation of the surroundings of HArF and HKrF molecules to more stable configurations. The vibrational frequency difference between the molecules in unstable and stable sites is very large for the H-Ng stretching mode: ~25 cm$^{-1}$ for HKrF and ~50 cm$^{-1}$ for HArF. The site conversion takes place at temperatures of ~27 and 31 K for HArF and HKrF, respectively.[38,61] This reorganization effect made studying the HArF and HKrF complexes with $N_2$ more complicated than HKrCl.

The H-Ng stretching modes of HArF and HKrF and their nitrogen complexes are presented in Figures 7 and 8. The monomer-to-complex shifts of these absorptions are presented in Table 5. Absorptions assigned to the HArF···$N_2$ complex were also seen in the HArF bending (680.3 and 702.9 cm$^{-1}$) and Ar-F stretching (431.7 cm$^{-1}$) regions. HKrF complex absorptions in the bending and Kr-F stretching regions were not observed.
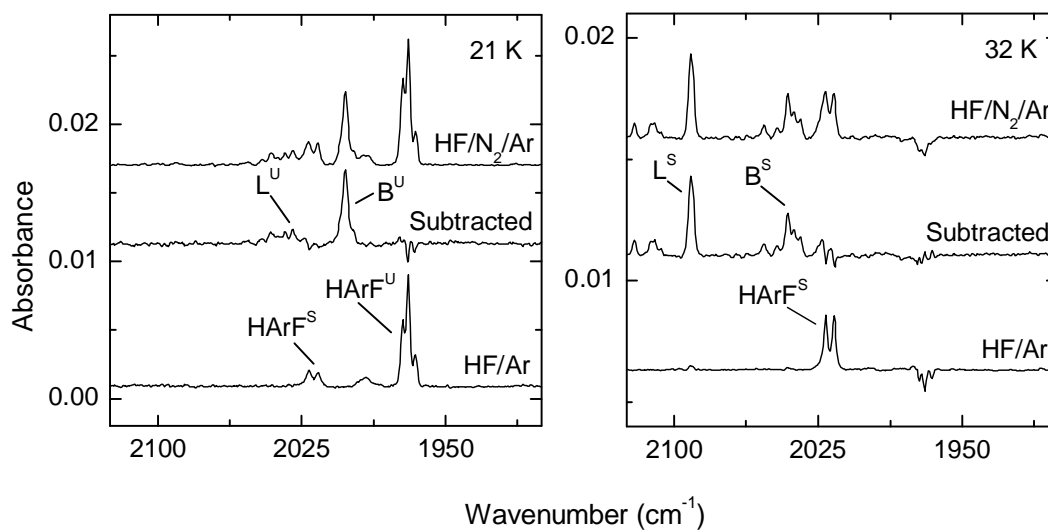
25

**Figure 7.** *FTIR spectra in the H-Ar stretching region of HArF and HArF···$N_2$ in solid argon. The spectra were measured at 8 K. The matrices are annealed at 21 and 32 K. The $N_2$ induced absorptions are assigned to the linear (L) and bent (B) complex structures of thermally stable (S) and unstable (U) HArF molecules.*
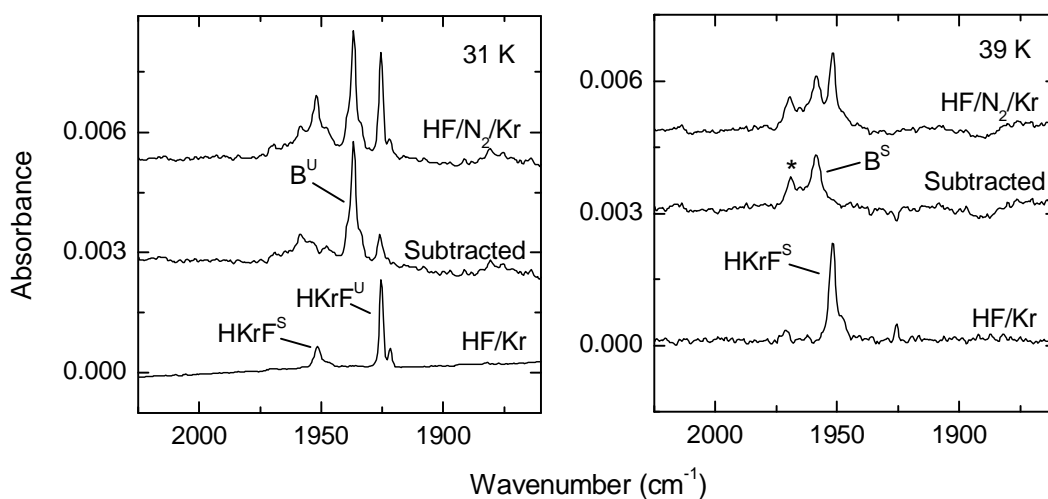


**Figure 8.** *FTIR spectra in the H-Kr stretching region of HKrF and HKrF···$N_2$ in solid krypton. The spectra were measured at 8 K. The matrices were annealed at 31 and 39 K. The $N_2$ induced absorptions are assigned to the bent (B) complex structure of thermally stable (S) and unstable (U) HKrF molecules. The band marked with an asterisk is either the linear complex or a second matrix site of the bent complex.*

The experimental monomer-to-complex shifts are in good agreement with the computations. The larger blue shifts can be connected to the linear complexes and the smaller shifts to the bent structures. Distinguishing between the complex structures of HArF⋯$N_2$ was quite straightforward. Conclusive assignment for HKrF$^S$⋯$N_2$ complexes was less certain. The experimental shift (+11.0 cm$^{-1}$) between the two HKrF$^S$⋯$N_2$ absorptions is quite small and the higher energy band (see asterisk in Fig. 8) may originate either from the linear complex or from the second matrix site of the bent structure.

### 5.2.2 HNgY⋯HX complexes

The photolysis and annealing of HBr/Xe, HCl/Xe and HBr/HCl/Xe matrices were studied. In these experiments, the concentration of HY dimer was optimized by adjusting the flow gas rate and deposition temperature. The HXeBr⋯HBr, HXeCl⋯HCl, and HXeCl⋯HBr complexes were identified using their intense H-Xe stretching vibration absorption. The formation of the complexes is presented in Figure 9.

The assignment of the HXeY⋯HX complexes is explained as follows. Upon photolysis of HY⋯HX (X,Y = Cl and Br) the Y⋯HX intermediate complexes appeared,[171,178] producing the precursors for the HXeY⋯HX complexes. The amount of HXeY⋯HX complex followed the intermediate complex concentration obtained during photolysis. The photostability of the HXeY monomers and complexes under UV radiation are similar (see Fig. 9). The computational predictions for the vibrational shifts are in good agreement with the experiments.
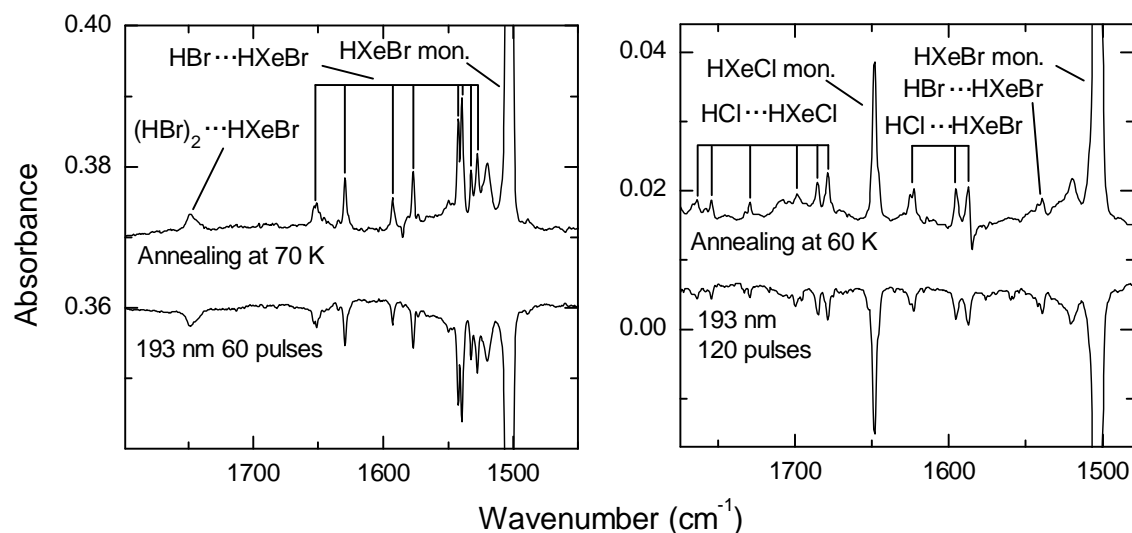


**Figure 9.** *FTIR spectra of HXeBr, HXeCl and their HX (X = Br and Cl) complexes in solid xenon at 8 K. The lower trace is the result of a short photolysis at 193 nm and indicates the bands that are due to HXeY-containing species.*

The experimental observations were limited to the H-Xe stretching region. The blue shifts obtained are from 24 to 148 cm$^{-1}$ for HXeBr···HBr, from 84 to 122 cm$^{-1}$ for HXeBr···HCl, and from 30 to 116 cm$^{-1}$ for HXeCl···HCl. Based on the computations, we have assigned blue shifts >70 cm$^{-1}$ to structure 1 and blue shifts <70 cm$^{-1}$ to structures 2 and 3 (see Fig. 2).

The interaction energies of complexes in the structure 1 configuration are about five times larger than those of complexes in structures 2 and 3. At low (<50 K) temperature annealings, the absorptions assigned to structure 1 have similar intensities to those of the other complexes. This indicates a thermodynamic non-equilibrium of complexes after photolysis and annealing. The intensities of the observed complex bands change after annealing at higher temperatures. New complex bands appear with small shifts (~20-30 cm$^{-1}$) and structure 1 is enhanced upon annealing at 70 K. This behavior is connected to thermal relaxation of the local matrix surroundings.

The structural assignments of the experimental absorptions are somewhat uncertain for to the following reasons. The computations refer to the gas phase systems while experiments are done in solid xenon. The HNgY molecules show strong solvation effects.[172,173] When forming a HXeY···HX complex, it should be taken into account that HNgY monomers are already in "complexed" form due to the surrounding matrix. Moreover, the complexes are formed in matrix cages that are not optimal to accommodate them i.e. the complex structures can differ substantially from the gas phase values.

**Table 5.**    *Experimental monomer-to-complex shifts (in cm$^{-1}$) of HNgY···N$_2$ and HXeY···HX complexes. The shifts are calculated from the strongest monomer absorptions of the H-Ng stretching mode.*

| HArF···N$_2$ | HKrF···N$_2$ | HKrCl···N$_2$ | HXeBr···HBr | HXeBr···HCl | HXeCl···HCl |
|---|---|---|---|---|---|
| +24.5 | +6.8 | +32.4 | +23.6 | +84.0 | +30.1 |
| +32.8 | +11.1 | +112.9 | +28.5 | +92.1 | +37.4 |
| +60.3 | +17.8 | | +35.3 | +119.1 | +50.2 |
| +75.1 | | | +38.6 | +121.5 | +80.8 |
| +95.3 | | | +73.3 | | +84.1 |
| +104.5 | | | +89.1 | | +106.4 |
| | | | +125.9 | | +115.5 |
| | | | +148.9 | | |
| | | | +245.4* | | |

*HXeBr···(HBr)$_2$ trimer (tentative assignment)

The vibrational blue-shifts of the H-Ng stretching vibrations seem to be the "normal" effect for the HNgY molecules. These shifts hold the record for blue-shifting H-bonds. Interestingly, van der Waals complexes (without H-bonding) also show substantial blue-shifts upon complexation. Indeed, vibrational blue-shifts have previously been attributed

only to H-bonded systems.[7,9] In addition to blue-shifted HNgY complexes, several examples of red-shifting HNgY complexes have been computationally predicted, but not found experimentally.[(Article IV), 127,128,157]

# 6. Interactions with the matrix

## 6.1. Matrix-site effect

The detailed vibrational band structure of HNgY molecules in noble-gas matrices was not discussed in early studies of these systems.[30,31,33,34] The HNgY molecules are embedded in a solid matrix and they interact with the surrounding atoms. In addition to the very large matrix-site splittings of HArF and HKrF,[38,61] many other HNgY molecules show smaller splittings in their band structures. Some of these molecules (e.g. HXeI, HXeBr, HXeCN, HXeSH, and HKrCN) show a characteristic band shape of a closely-spaced pair of bands and a relatively weak broader satellite at higher energy.[30,31,174,175]

The main band of HXeBr is split into a doublet. The intensities of these absorptions depend on the annealing time, with longer annealing times enhancing the $S_1$ satellite (see Fig. 10). Matrix deposition temperature has a noticeable effect on the HXeBr main band structure and deposition at lower temperatures broadens the HXeBr bands. After depositions at 10-25 K, the $S_1/S_2$ doublet is not resolved even after annealing at 35 K, but annealing at higher temperatures (60 K) restores the $S_1/S_2$ doublet. This band structure was assigned to HXeBr in different matrix sites.[Article V]
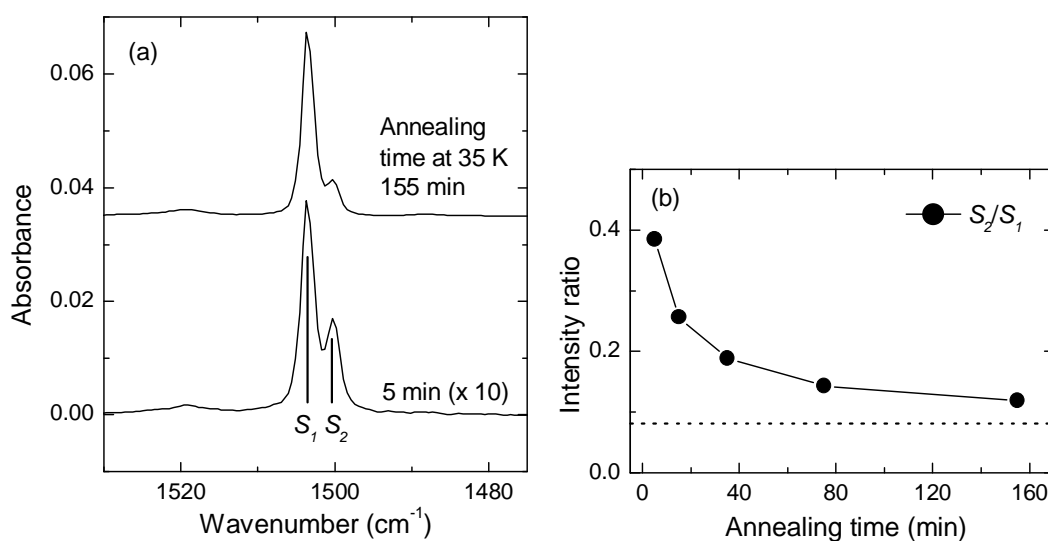


**Figure 10.** *(a) FTIR spectra of the H-Xe stretching vibration of HXeBr in a xenon matrix after different annealing periods at 35 K. The $S_1$ and $S_2$ bands originate from HXeBr in two matrix sites. The spectra were measured at 8 K. (b) $S_1/S_2$ intensity ratios as a function of annealing time at 35 K. The dotted line represents the $S_1/S_2$ intensity ratio obtained after annealing at 45 K.*

The HXeBr matrix site splitting was modelled with computational 1:1 Xe···HXeBr complexes (see Fig. 3). The calculations show that the H-Xe vibrational frequency can vary by several cm$^{-1}$ in different Xe···HXeBr structures (see Table 2). These interaction-induced shifts agree with the experimental interval of ~3 cm$^{-1}$ between the $S_1$ and $S_2$ absorptions. This is in accordance with the computational simulations of HArF by Jolkkonen et al.: they suggested that the band splitting of HArF is caused by a specific interaction between one surrounding argon atom and the HArF molecule.[176] The matrix-site structure of HArF molecules has also been studied by Bihary et al. and Bochenkova et al..[177,178] The most successful method for explaining the band structure of HArF seems to be the DIM based QM/MM method used by Bochenkova et al.,[178] but they did not find evidence for any specific interaction between HArF and argon atoms. Thus, the question of specific interactions in noble-gas matrices remains open.

## 6.2. Librational motion

The spectra of HXeBr and HKrCl were measured at different temperatures and a temperature dependence of the vibrational band satellites $L_1$ and $L_2$ was found (see Fig. 11 and Table 6). A model explaining the common features of the temperature dependent processes was developed. These temperature dependent absorptions were connected to the hindered rotation (libration) of HXeBr and HKrCl in a noble-gas matrix.

The $L_1$ band is relatively strong at lower temperatures and the $L_2$ band rises at higher temperatures. This thermal process is fully reversible and the shifts of the $L_1$ and $L_2$ bands from the main absorption band are practically equal. The vibrational frequencies of HXeBr and HKrCl are collected in Table 6.

**Table 6.** *H-Ng stretching absorptions of HXeBr and HKrCl with librational fine structure ($L_1$, $L_2$).*

|  | non-librating | $L_1$ | $L_2$ |
|---|---|---|---|
| HXeBr | 1503.7 *(S₁)*, 1500.2 *(S₂)* | 1519.6 | 1486.8 |
| HKrCl | 1476.2 | 1496.0 | 1456.4 |

The librational band structure of HKrCl and HXeBr was simulated by a simple phenomenological approach developed by Flygare and later adapted by Apkarian and Weitz.[179,180] Reasonable agreement with experiments was obtained by tuning the interaction strength. Examples of the simulated librational spectra of HXeBr at two temperatures are presented in Figure 12(a). The temperature dependences of computational and experimental $L_1/L_2$ intensity ratios are presented in Figure 12(b).
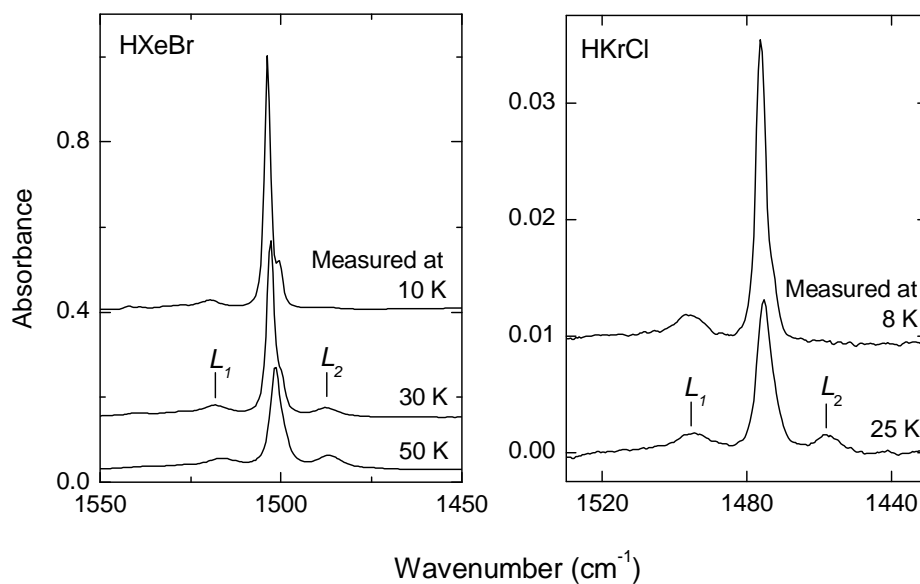
**Figure 11.** *FTIR spectra of the H-Ng stretching absorptions of HXeBr in solid xenon and HKrCl in solid krypton measured at different temperatures. The bands marked with $L_1$ and $L_2$ are explained by the librational motion of these molecules in the surrounding noble-gas hosts.*
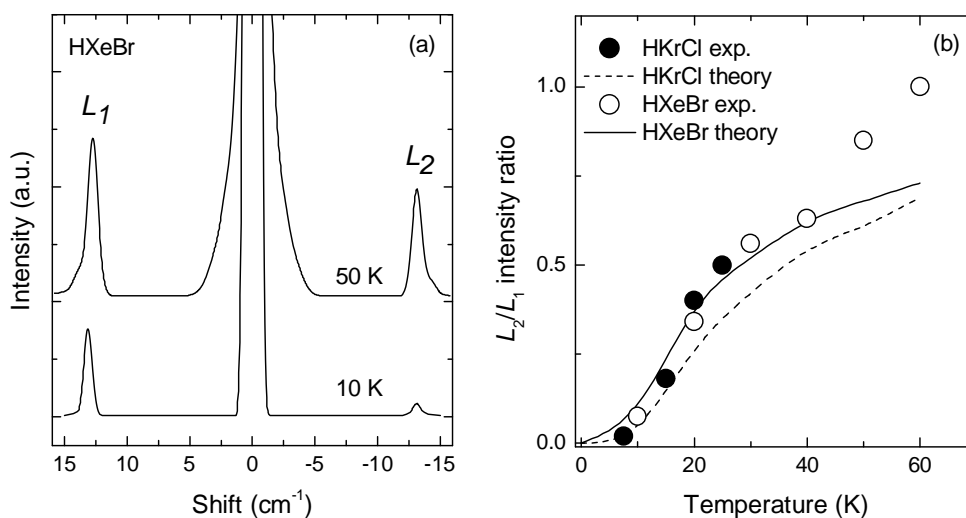


**Figure 12.** *(a) Simulated librational satellites of HXeBr in a xenon matrix at 10 K and 50 K. (b) Intensity ratios of librational satellites $L_1$ and $L_2$ as a function of matrix temperature. Circles represent the experimental data and lines are the simulations.*

An alternative explanation for the $L_1$ and $L_2$ bands is the interaction of the HNgY molecule with lattice phonons. This is less probable than libration, because the phonon bands should be broad and the absorptions should be activated up to the Debye frequency of the lattice (~50 and 45 cm$^{-1}$ for Kr and Xe, respectively) as demonstrated for formic acid in noble-gas matrices.[181] The experimental bands are narrow <10 cm$^{-1}$ and they are separated by ~15 and 20 cm$^{-1}$ from the main spectral bands of HXeBr and HKrCl, respectively.

Recently, the librational motion of HArF in solid argon was studied experimentally and computationally.[42] The theoretical approach used by Bochenkova et al. successfully explained the experimental observations of HArF libration. This work further confirms the assignment of the $L_1$ and $L_2$ bands of HXeBr and HKrCl to librational motion. The theoretical approach used by Bochenkova et al. could be used to simulate the libration of other HNgY molecules as well, but the method is very demanding.

## 6.3. Energetic stabilization by intermolecular interactions

The HHeF molecule is the first computationally predicted candidate for a chemical compound of helium.[51-55] The life-time of HHeF is limited by tunneling over pico- to femtosecond timescales.[52,53] It is valuable to study possible methods to stabilize HHeF and so the solvation of HHeF in a xenon cluster was modeled. This complexation (solvation) induced stabilization of the HHeF molecule might be a means of enhancing its life-time and aiding in its experimental observation. The computed structures of HHeF···(Xe)$_n$ ($n$ = 1-6) are presented in Figure 13.



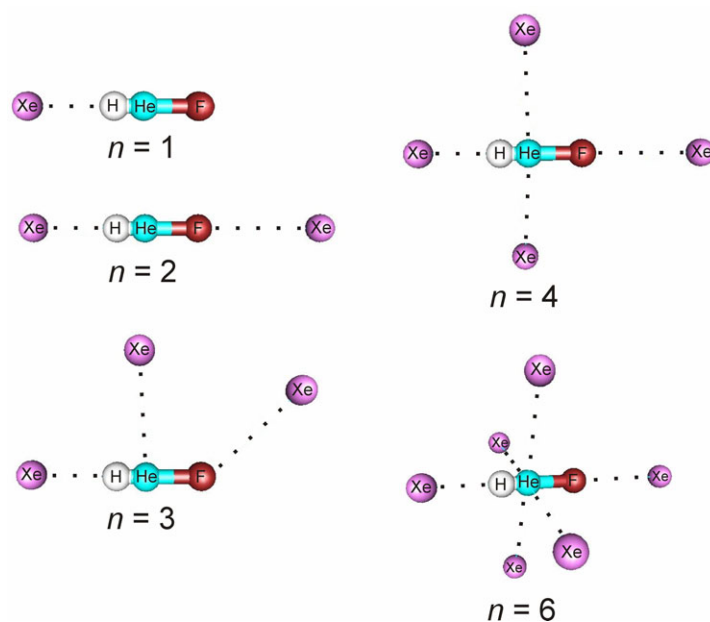**Figure 13.** *Computational structures of the HHeF···Xe$_n$ complexes at the MP2/6-311++G(2d,2p), SDD (Xe atom) level of theory.*

33

According to calculations, HHeF is higher in energy than the corresponding H + He + F neutral fragments and its life-time is limited by tunneling through the bending and stretching barriers.[52,53] Figure 14(a) shows the schematic potential-energy surface of HHeF. An interesting possibility is the energetic stabilization of the HHeF molecule below the atomic asymptote through complexation with another species. This would have two important consequences. First, this might make possible the preparation of HHeF using the diffusion controlled H + He + F reaction. Second, this suppresses the tunneling via stretching, hence increasing the HHeF life-time. The energetic stabilization of HHeF by xenon atoms is presented in Figure 14(b). It is seen that the preparation of HHeF in a Xe matrix could increase its lifetime by lowering its energy. It has been previously suggested that high pressures can increase the lifetime of HHeF.[54]
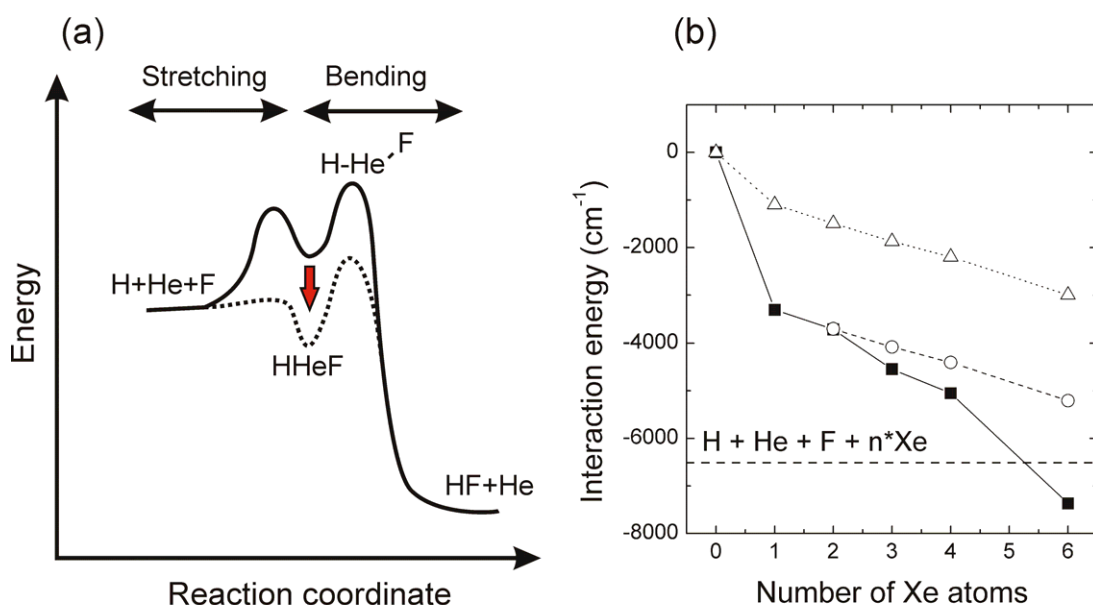


**Figure 14.** *(a) Schematic potential energy surface of HHeF presenting its stretching and bending coordinates. The red arrow shows an idealistic effect of complexation stabilizing HHeF below its atomic asymptote (energy difference ~6500 cm$^{-1}$).$^{(Article III)}$ (b) Total interaction energies of the HHeF$\cdots$Xe$_n$ complexes are represented by solid squares. The stabilization energy corrected with Xe-Xe interactions is shown by open circles. Triangles show the stabilization energy after making the BSSE and Xe-Xe interaction corrections.*

The study of HHeF$\cdots$Xe$_n$ ($n$ = 1-6) shows that it is improbable that the HHeF$\cdots$Xe$_6$ cluster brings the HHeF molecule below the atomic asymptote. However, as a working hypothesis, the stabilization effect can continue for larger xenon clusters. It would be valuable to consider the situation in bulk xenon. A particle in a single-substitutional site of a xenon crystal has 12 closest neighbor atoms. It is possible that HHeF becomes lower in energy than the atomic fragments in large xenon clusters. The treatment of HHeF in a matrix is a complicated computational task.

# 7. YHY⁻···N₂ and NgHNg⁺···N₂ complexes

## 7.1. Computational results

For NgHNg⁺···N₂ complexes, two energy minima on the potential energy surface were found and they are named linear and T-shaped structures. The YHY⁻···N₂ complexes also show two energy minima: a cross-like structure for both anions, and a linear structure for ClHCl⁻···N₂ and a T-shaped structure for BrHBr⁻···N₂. The computational structures are presented in Figure 15.
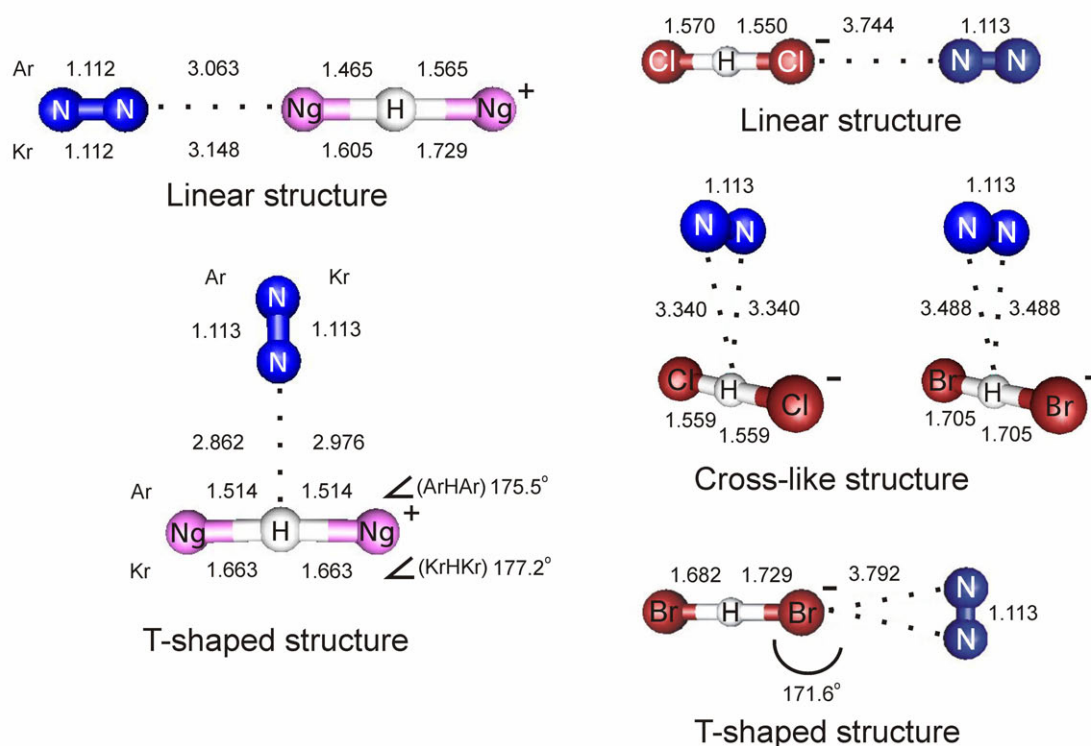


**Figure 15.** *Optimized structures of the NgHNg⁺···N₂ and YHY⁻···N₂ complexes at the MP2/6-311++G(2d,2p) level of theory. The bond lengths are in Å. The data for Ng = Ar and Kr are indicated in the figure.*

The linear geometry of the NgHNg⁺···N₂ and BrHBr⁻···N₂ complexes changes the $D_{\infty h}$ symmetry to $C_{\infty v}$, which activates the symmetric stretching absorption. For the T-shaped and cross-like structures, the degeneracy of the bending vibration breaks, leading to two different bending frequencies. The computational vibrational data is collected in Table 7.

The BSSE corrected interaction energies of the YHY⁻···N₂ and NgHNg⁺···N₂ complexes are presented in Table 8. Both the linear and the T-shaped structures of the NgHNg⁺···N₂ complexes are bound by ~1000 cm⁻¹. For the YHY⁻···N₂ complexes, the cross-like structures are more strongly bound and the linear ClHCl⁻···N₂ complex has a positive interaction energy suggesting that it is energetically unstable.

**Table 7.** *Computational vibrational frequencies and monomer-to-complex vibrational shifts (in cm$^{-1}$) of NgHNg$^+$ and YHY$^-$ monomers and their N$_2$ complexes. The level of theory is MP2/6-311++G(2d,2p). The IR absorption intensities (in km mol$^{-1}$) are given in parentheses.*

| | $\nu_3$ | shift $\nu_3$ | $\nu_2$ | $\nu_1$ |
|---|---|---|---|---|
| **ArHAr$^+\cdots$N$_2$** | | | | |
| monomer | 1028.2 (5160) | – | 694.2 (104) | 318.8 (0) |
| linear | 1096.6 (5462) | +68.4 | 716.7 (105) | 305.0 (62) |
| T-shaped | 1011.0 (4876) | −17.2 | 654.3 (80), 705.5 (47) | 315.8 (0) |
| **KrHKr$^+\cdots$N$_2$** | | | | |
| monomer | 925.4 (6026) | – | 664.5 (43) | 206.1 (0) |
| linear | 1017.6 (6296) | +92.2 | 680.1 (44) | 192.2 (48) |
| T-shaped | 927.9 (5768) | +2.5 | 652.2 (34), 677.4 (19) | 206.0 (0) |
| **BrHBr$^-\cdots$N$_2$** | | | | |
| monomer | 667.1 (7938) | – | 748.0 (2) | 207.3 (0) |
| cross-like | 675.4 (7594) | +8.3 | 755.5 (1), 748.2 (0) | 207.8 (0) |
| T-shaped | 688.5 (8095) | +21.4 | 763.3 (2), 754.1 (2) | 205.2 (0) |
| **ClHCl$^-\cdots$N$_2$** | | | | |
| monomer | 690.8 (7080) | – | 869.4 (11) | 343.6 (0) |
| cross-like | 700.5 (6721) | +9.7 | 870.6 (11), 864.2 (6) | 344.4 (0) |
| linear | 696.1 (7379) | +4.8 | 880.7 (12) | 342.6 (21) |

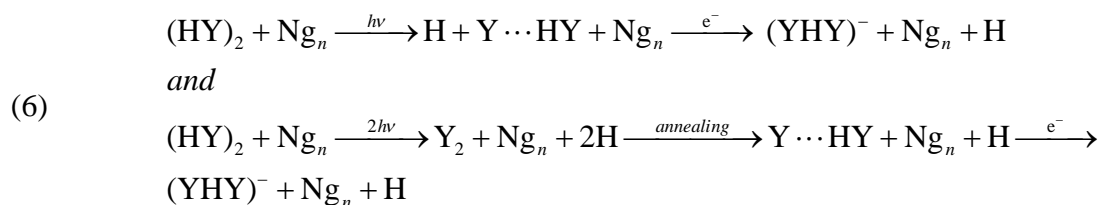**Table 8.** *BSSE-corrected interaction energies (in cm$^{-1}$) of the NgHNg$^+\cdots$N$_2$ and YHY$^-\cdots$N$_2$ complexes at the MP2/6-311++G(2d,2p) level of theory.*

| | ArHAr$^+\cdots$N$_2$ | KrHKr$^+\cdots$N$_2$ | | BrHBr$^-\cdots$N$_2$ | | ClHCl$^-\cdots$N$_2$ |
|---|---|---|---|---|---|---|
| linear | −927 | −935 | cross-like | −520 | linear | −559 |
| T-shaped | −1176 | −996 | T-shaped | −338 | cross-like | +77 |

## 7.2. Experimental results and discussion

The photolysis of hydrogen containing molecules in noble-gas matrices leads to charge transfer processes where a hydrogen atom can trap the positive charge (react with a hole) to form the NgHNg$^+$ cation.[69-73] In addition to NgHNg$^+$ cations, the formation of YHY$^-$ (Y = halogen atom) anions takes place in HY/Ng matrices upon photolysis and annealing.[79-84] The formation of YHY$^-$ is mainly obtained after annealing at temperatures close to the diffusion temperature of a hydrogen atom.[182-184] The formation process probably involves

the reaction of a hydrogen atom with a halide molecule. The possible mechanisms for the formation of these ionic species are described as follows:

(5)
$$\mathrm{HY} + \mathrm{Ng}_n \xrightarrow{h\nu} \mathrm{Y} + \mathrm{Ng}_n + \mathrm{H} \xrightarrow{h\nu} \mathrm{Y}^- + \mathrm{Ng}_n^+ + \mathrm{H} \longrightarrow$$
$$\mathrm{Y}^- + \mathrm{Ng}_{n-2} + (\mathrm{NgHNg})^+$$

(6)
$$(\mathrm{HY})_2 + \mathrm{Ng}_n \xrightarrow{h\nu} \mathrm{H} + \mathrm{Y} \cdots \mathrm{HY} + \mathrm{Ng}_n \xrightarrow{e^-} (\mathrm{YHY})^- + \mathrm{Ng}_n + \mathrm{H}$$
*and*
$$(\mathrm{HY})_2 + \mathrm{Ng}_n \xrightarrow{2h\nu} \mathrm{Y}_2 + \mathrm{Ng}_n + 2\mathrm{H} \xrightarrow{annealing} \mathrm{Y} \cdots \mathrm{HY} + \mathrm{Ng}_n + \mathrm{H} \xrightarrow{e^-}$$
$$(\mathrm{YHY})^- + \mathrm{Ng}_n + \mathrm{H}$$
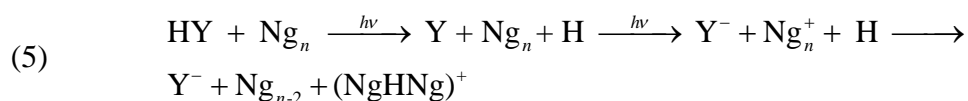
In the $\mathrm{HY/N_2/Ng}$ experiments, additional absorptions, shifted to the blue from the $\mathrm{YHY}^-$ and $\mathrm{NgHNg}^+$ bands, are observed. These new bands are assigned to nitrogen complexes of these ionic species. Figure 16 presents the absorption spectra of $\mathrm{ClHCl}^-$, $\mathrm{BrHBr}^-$ and their $\mathrm{N_2}$ complexes. The $\mathrm{YHY}^- \cdots \mathrm{N_2}$ complexes rise synchronously with $\mathrm{YHY}^-$ ions upon annealing at 20 and 30 K in argon and krypton matrices, respectively. Figure 17 shows the $\mathrm{N_2}$ complexes of the $\mathrm{ArHAr}^+$ and $\mathrm{KrHKr}^+$ cations. The $\mathrm{NgHNg}^+$ absorptions are independent of precursor molecule (HCl and HBr). The cations and their complexes decompose upon annealing as shown in Figure 17. The main spectral features are the antisymmetric stretching modes. The anharmonicity of the $\mathrm{YHY}^-$ and $\mathrm{NgHNg}^+$ ions leads to strong coupling between the symmetric ($\nu_1$) and antisymmetric ($\nu_3$) vibrations, building up the intense combination bands.[69,70,185] The $\mathrm{N_2}$ complex bands of $\mathrm{ArHAr}^+$, $\mathrm{KrHKr}^+$, and $\mathrm{BrHBr}^-$ were also detected in the combination vibration region. The vibrational frequencies of these ions and their complexes are collected in Table 9.

**Table 9.**　　*Experimental absorptions (in cm$^{-1}$) of ArHAr$^+$, KrHKr$^+$ and their N$_2$ complexes.*

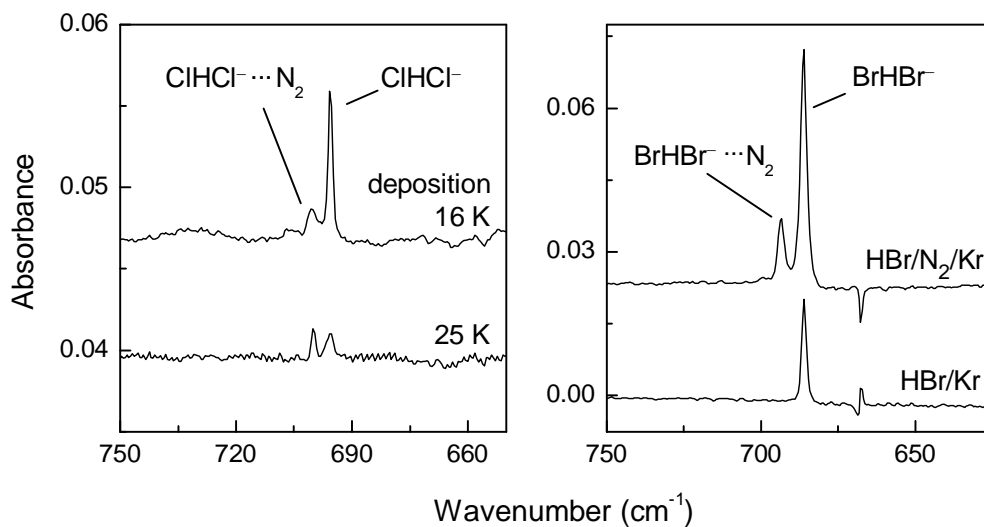|  | ArHAr$^+$ | ArHAr$^+\cdots$N$_2$ | KrHKr$^+$ | KrHKr$^+\cdots$N$_2$ | ClHCl$^-$ | ClHCl$^-\cdots$N$_2$ | BrHBr$^-$ | BrHBr$^-\cdots$N$_2$ |
|---|---|---|---|---|---|---|---|---|
| $\nu_3$ | 903.0 | 928.5 | 852.6 | 863.0 | 695.5 | 700.3 | 686.3 | 693.3 |
| $\nu_3+\nu_1$ | 1139.2 | 1183.6 | 1008.0 | 1020.5 | 954.9 | – | 844.8 | 865.8 |

**Figure 16.** *FTIR spectra of ClHCl⁻ and BrHBr⁻ in Ar and Kr, respectively, and their N₂ complexes. The higher deposition temperature increases the relative concentration of the YHY⁻···N₂ complexes as demonstrated for ClHCl⁻.*
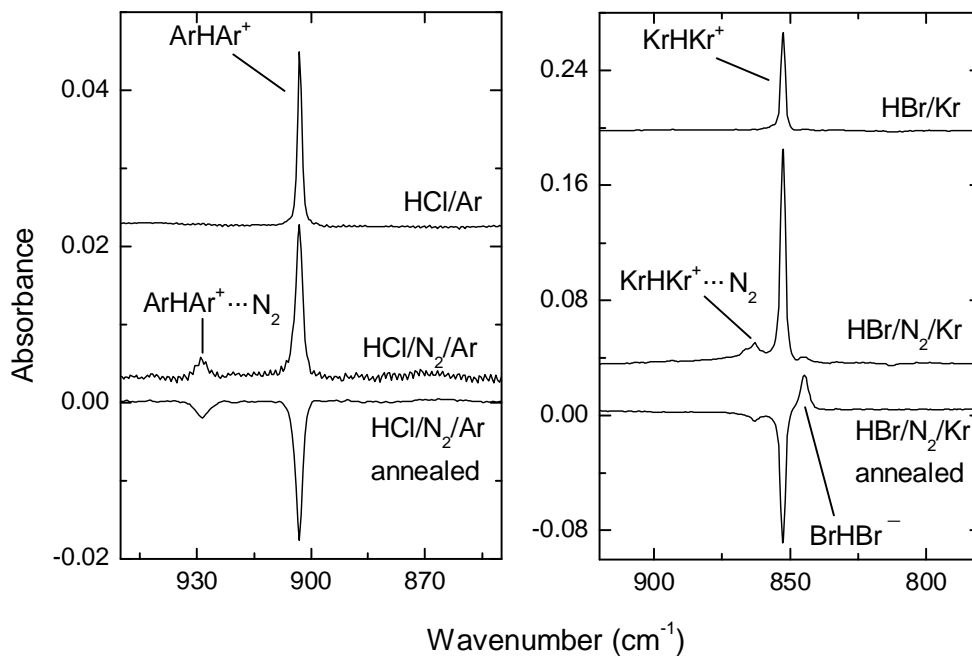


**Figure 17.** *FTIR spectra of ArHAr⁺ and KrHKr⁺ monomers in Ar and Kr matrices, respectively (upper traces), and their N₂ complexes (middle traces). The lower trace shows the effect of annealing at 30 K (Ar) and 35 K (Kr).*

## 7.3. Formation of YHY⁻ and decay of NgHNg⁺ ions

The formation and decay of NgHNg⁺ and YHY⁻ ions are interesting solid-state phenomena and these relatively simple systems can help us to understand solid-state charge-transfer processes.[73] The mechanism for the decay of NgHNg⁺ ions in matrices has been discussed and several mechanisms for this process have been suggested. The room-temperature black-body radiation assisted tunneling of a proton has been suggested by Beyer *et al.* and this could explain some previous experimental observations.[77,78] Based on the present data, a new model of the electron tunneling mechanism for the decay process is suggested.

It was found in Article V that the stabilities of ArHAr⁺ and KrHKr⁺ ions are quite comparable, while Bondybey *et al.* reported a four-fold larger stability of KrHKr⁺ compared to ArHAr⁺.[65,71] In fact, their theoretical models suggested that the size of this difference should be several orders of magnitude.[65,71] The decay of NgDNg⁺ is clearly seen in our experiments (see Fig. 18) and it does not fit the theoretical six-seven orders of magnitude difference between the H⁺ and D⁺ tunneling rate.[77,78]
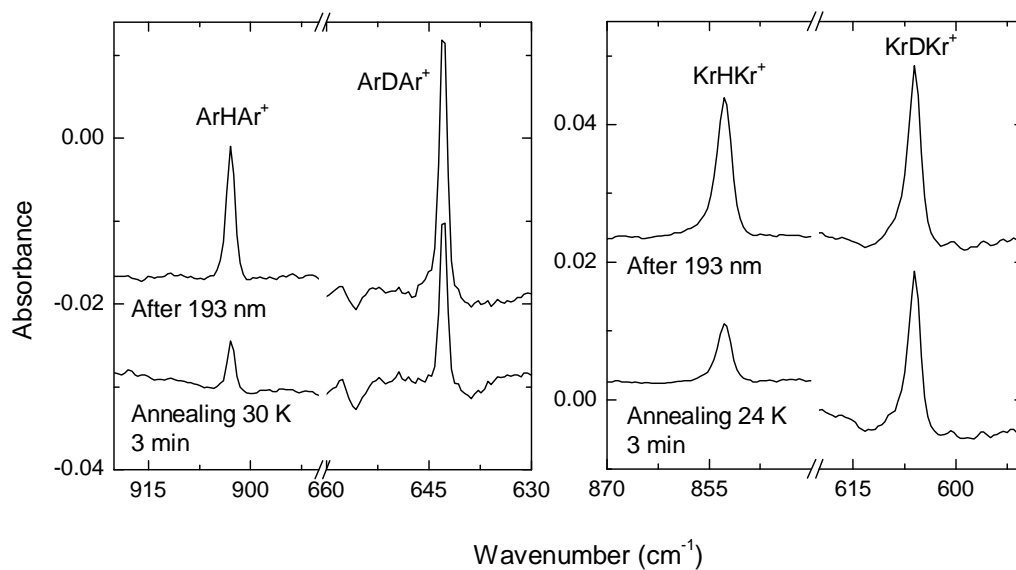


**Figure 18.** *Protons and deuterons solvated in argon and krypton matrices. The spectra correspond to the situations after photolysis of HF(DF)/Ar and HF(DF)/Kr matrices and after annealing the photolyzed matrix.*

Upon annealing, the YHY⁻ concentration increases (see Fig. 19) which seems to contradict the proton diffusion model. It would be natural to expect bleaching of the negative charges upon global mobility of protons due to neutralization reactions, but the opposite effect is observed. The black-body radiation assisted mobility of protons can also

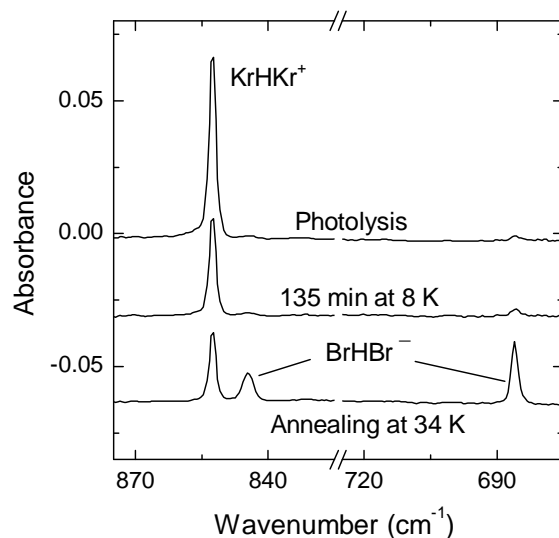be ruled out since the decay rates of NgHNg$^+$ ions were quite similar under glowbar radiation and in darkness.



**Figure 19.** *KrHKr$^+$ and BrHBr$^-$ in a krypton matrix. Shown are (from top to bottom) the spectra after 193 nm photolysis, after 135 min at 8 K, and after annealing the sample at 34 K for 3 min.*

These experimental findings suggest an alternative model for the decomposition of NgHNg$^+$. In this model, the decomposition of cations is explained by their reactions with electrons stored in the matrix as a result of photolysis. The transfer of electrons in matrices most probably takes place via a tunneling mechanism. The neutralization of the NgHNg$^+$ fragments by electrons is an exothermic process,[71,89] and electron tunneling over long distances is a known physical phenomenon in solid matrices.[186-189] The electron tunneling mechanism also explains the observed increase of YHY$^-$ absorptions upon annealing. A schematic picture of the electron tunneling processes is presented in Figure 20.

In the proton-diffusion mechanism, the decay kinetics of the relatively strongly bound NgHNg$^+\cdots$N$_2$ complexes should be different to that of the corresponding monomers. According to the Fermi golden rule,[190-193] proton tunneling in a symmetrical potential well (with the same initial and final tunneling states) can take place [see Fig. 21(a)]. For the NgHNg$^+\cdots$N$_2$ complexes, the initial (complexed) and final (uncomplexed) vibrational states have different energies and this makes the tunneling of a proton improbable at low matrix temperatures. The energy of these states differs by the complex interaction energy and the complexed form is lower in energy. Under these circumstances, it would be plausible to expect rather an increase of the NgHNg$^+\cdots$N$_2$ concentration upon annealing due to the hypothetical mobile protons.

In the present study, the synchronous decay of $NgHNg^+$ and its $N_2$ complex is observed [see Fig 21(c)]. This suggests immobility of protons in noble-gas matrices and supports the electron tunneling mechanism, suggested in Article V and presented in Figure 20. This question remains a challenge for further studies.
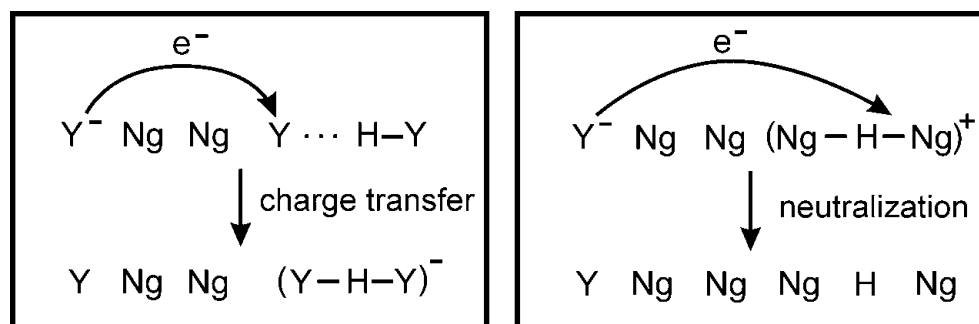


**Figure 20.** *Schematic electron tunneling mechanism for the decomposition of $NgHNg^+$ and the formation of $YHY^-$ in noble-gas matrices.*
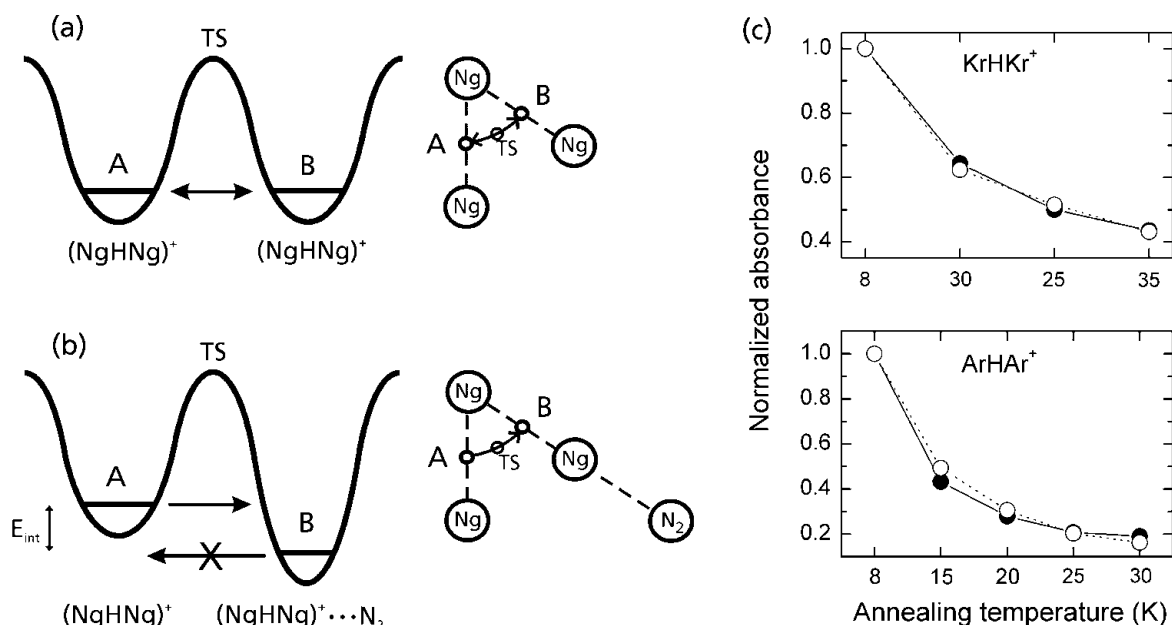


**Figure 21.** *Schematic view of potential energy surfaces for hypothetical proton diffusion of (a) the $NgHNg^+$ monomer and (b) the $NgHNg^+ \cdots N_2$ complex. The tunneling induced diffusion of a proton can in principle take place, but it should be suppressed at low temperatures for the $N_2$ complex. TS is the transition state between the energy minima A and B. (c) Relative intensities of $NgHNg^+$ and its $N_2$ complex as a function of annealing temperature. Open and solid circles represent monomers and complexes, respectively. Similar decay of the complexed and monomeric species contradicts the hypothetical tunneling-assisted diffusion of protons.*

41

The electron trap in matrices is most probably the electronegative Y fragment produced by photolysis of HY. It is difficult to detect these $Y^-$ fragments using IR spectroscopy and thus it is also difficult to observe the correlation between the decay of $Y^-$ and $YHY^-$ formation and the neutralization of $NgHNg^+$. In a recent study,[194,195] it was found that the decays of the $CCCN^-$ and $NgHNg^+$ cations are synchronous. Additionally, the formation of a species tentatively assigned as the CCCN radical was observed during this process. These recent findings support the electron tunneling model for the charge transfer processes. A less likely electron trap would be a noble-gas lattice solvated electron.[196-198]

# 8. Conclusions in brief

In this work, a number of intermolecular interactions of different species were computationally and experimentally studied. These interactions include molecular complexes, interactions with the surrounding matrix (matrix site effect), and librational motion. The model proposed here explains all of the IR spectral features of the HNgY molecules.

A number of noble-gas-hydride complexes were studied experimentally and computationally. These complexes show many unusual features e.g. the large blue shifts of their H-Ng stretching vibration frequency upon complexation. Record-braking blue-shift values were observed. The blue shifts of these molecules were explained by the enhanced $(HNg)^+Y^-$ ion-pair nature upon complex formation. HNgY complexes are the first step towards the production of these molecules in clusters and in crystalline form. The HXeH and HXeCCH crystals are computationally predicted.[63,64]

Whether or not the HNgY species exist under normal conditions is an open question. It is possible that the stabilization of HNgY species upon complexation is a step towards the answer. The geophysical problem of missing xenon is also relevant here.[199,200] The preparation of helium and neon compounds is discussed with respect to complexation-induced stabilization. In particular, the complexation-induced stabilization of the hypothetical HHeF molecule is discussed in this thesis.

The formation and decay of centrosymmetic $YHY^-$ (Y = halogen atom) and $NgHNg^+$ (Ng = noble-gas atom) ions was studied and a new electron tunneling mechanism for these processes was suggested. The $N_2$ complex formation of these ions was demonstrated and the $NgHNg^+$ complex studies further support the electron tunneling mechanism.

# References

1       G. C. Pimentel and A. L. McLellan, *The Hydrogen Bond*, W. H. Freeman and Co., San Francisco (1960).

2       G. R. Desiraju and T. Steiner, *The Weak Hydrogen Bond*, Oxford University Press, Oxford (1999).

3       G. A. Jeffrey, *Hydrogen Bonding in Biological Structures*, Springer, Berlin (1991).

4       H. E. Hallam (ed.), *Vibrational Spectroscopy of Trapped Species*, John Wiley & Sons, Bristol (1973).

5       L. Andrews and M. Moskovits (ed.), *Chemistry and Physics of Matrix-Isolated Species*, Amsterdam (1989).

6       S. Scheiner, *Hydrogen Bonding*, Oxford University Press, New York (1997).

7       P. Hobza and Z. Havlas, *Chem. Rev.* **100**, 4253 (2000).

8       K. Hermansson, *J. Phys. Chem. A* **106**, 4695 (2002).

9       A. J. Barnes, *J. Mol. Struct.* **704**, 3 (2004).

10      E. S. Kryachko in *Hydrogen Bonding ‐ New Insights,* edited by S. J. Grabowski, Springer, Dordrecht (2006), Chapter 8.

11      J. Joseph and E. D. Jemmis, *J. Am. Chem. Soc.* **129,** 4620 (2007).

12      S. Pinchas, *Anal. Chem.* **27**, 2 (1955).

13      S. Pinchas, *Anal. Chem.* **29**, 334 (1957).

14      S. Pihchas, *Chem. Ind.* (London) 1451 (1959).

15      S. Pinchas, *J. Phys. Chem.* **67**, 1862 (1964).

16      S. L. Paulson and A. J. Barnes, *J. Mol. Struct.* **80**, 151 (1982).

17      M. Buděśínský and P. Fiedler, Z. Arnold, *Synthesis (Stuttgart)* **11**, 858 (1989).

18      P. Hobza, V. Śpirko, Z. Havlas, K. Buchhold, B. Reimann, H.-D. Barth, and B. Brutschy, *Chem. Phys. Lett.* **299**, 180 (1999).

19      B. Reimann, K. Buchhold, S. Vaupel, B. Brutchky, Z. Havlas, V. Śpirko, and P. Hobza, *J. Phys. Chem. A*, **105**, 5560 (2001).

20      P. Hobza, *Phys. Chem. Chem. Phys.* **3**, 2555 (2001).

21      P. Hobza and Z. Havlas, *Theor. Chem. Acc.* **108**, 325 (2002).

22      X. Li, L. Liu, and H. B. Schlegel, *J. Am. Chem. Soc.* **124**, 9639 (2002).

23      L. Pejov and K. Hermansson, *J. Chem. Phys.* **119,** 313 (2003).

24      I. V. Alabugin, M. Manoharan, S. Peabody, and F. Weinhold, *A. Am. Chem. Soc.* **125**, 5973 (2003).

25      W. Zierkiewicz, P. Jurecja, and, P. Hobza, *Chem. Phys. Chem.* **6**, 609 (2005).

26      L. Pauling, *J. Am. Chem. Soc.* **55**, 1895 (1933).

27      N. Bartlett, *Proc. Chem. Soc. London*, 218 (1962).

28      J. J. Turner and G. C. Pimentel, *Science* **140**, 975 (1963).

29      V. V. Avrorin, R. N. Krasikova, V. D. Nefedov, and M. A. Toropova, *Russ. Chem. Rev.* **51**, 12 (1982).

30      M. Pettersson, J. Lundell, and M. Räsänen, *J. Chem. Phys.* **102**, 6423 (1995).

31      M. Pettersson, J. Lundell, and M. Räsänen, *J. Chem. Phys.* **103**, 205 (1995).

32      K. O. Christe, *Angew. Chem. Int. Ed.* **40**, 1419 (2001).

33      M. Pettersson, J. Lundell, and M. Räsänen, *Eur. J. Inorg. Chem.*, **729** (1999).

34      J. Lundell, L. Khriachtchev, M. Pettersson, and M. Räsänen, *Low Temp. Phys.* **26**, 680 (2000).

35      R. B. Gerber, *Ann. Rev. Phys. Chem.* **55**, 55 (2004).

36      M. Pettersson, L. Khriachtchev, J. Lundell, and M. Räsänen, in *Inorganic Chemistry in Focus II,* edited by G. Meyer, D. Naumann, and L. Wesemann, Wiley-VCH, Weinheim (2005), pp. 15-34.

37      L. Khriachtchev, M. Pettersson, N. Runeberg, J. Lundell, and M. Räsänen, *Nature (London)* **406**, 874 (2000).

38      L. Khriachtchev, M. Pettersson, A. Lignell, and M. Räsänen, *J. Am. Chem. Soc.* **123**, 8610 (2001).

39      L. Khriachtchev, A. Lignell, and M. Räsänen, *J. Chem. Phys.* **120**, 3353 (2004).

40      L. Khriachtchev, A. Lignell, and M. Räsänen, *J. Chem. Phys.* **123**, 064507 (2005).

41      A. Lignell, L. Khriachtchev, M. Pettersson, and M. Räsänen   *J. Chem. Phys.* **118**, 11120 (2003).

42    A. V. Bochenkova, L. Khriachtchev, A. Lignell, M. Räsänen, H. Lignell, A. A. Granovsky, and A. V. Nemukhin, *Phys. Rev. B* **77**, 094301 (2008).

43    M. Johansson, M. Hotokka, M. Pettersson, and M. Räsänen, *Chem. Phys.* **244**, 25 (1999).

44    J. Lundell, G. M. Chaban, and R. B. Gerber, *Chem. Phys. Lett.* **331**, 308 (2000).

45    N. Runeberg, M. Pettersson, L. Khriachtchev, J. Lundell, and M. Räsänen, *J. Chem. Phys.* **114**, 836 (2001).

46    S. Berski, B. Silvi, J. Lundell, S. Noury, and Z. Latajka, in *New Trends in Quantum Systems in Chemistry and Physics,* edited by J. Maruani, C. Minot, R. McWeeny, Y. G. Smeyers, and S. Wilson, Kluwer Academic Publishers, Dordrecht (2001), pp. 259-279.

47    G. M. Chaban, J. Lundell, and R. B. Gerber, *Chem. Phys. Lett.* **364**, 628 (2002).

48    J. Lundell, A. Cohen, and R. B. Gerber, *J. Phys. Chem. A* **106**, 11950 (2002).

49    A. Lignell, L. Khriachtchev, J. Lundell, H. Tanskanen, and M. Räsänen, *J. Chem. Phys.* **125**, 184514 (2006).

50    T. Takayanagi, T. Asakura, K. Takahashi, Y. Taketsugu, T. Tagetsugu, and T. Noro, *Chem. Phys. Lett* **446**, 14 (2007).

51    M. W. Wong, *J. Am. Chem. Soc.* **122**, 6289 (2000).

52    G. M. Chaban, J. Lundell, and R. B. Gerber, *J. Chem. Phys.* **115**, 7341 (2001).

53    T. Takayanagi and A. Wada, *Chem. Phys. Lett* **352** 91 (2002).

54    Z. Bihary, G. M. Chaban, and R. B. Gerber, *J. Chem. Phys.* **117** 5105 (2002).

55    T. Takayanagi, *Chem. Phys. Lett* **371**, 675 (2003).

56    A. Lignell, J. Lundell, M. Pettersson, L. Khriachtchev, and M. Räsänen, *Low Temp. Phys.* **29**, 844 (2003) [originally *Fiz. Niz. Temp.* **29**, 1109 (2003)].

57    R. Baumfalk, N. H. Nahler, and U. Buck, *J. Chem. Phys.* **114**, 4755 (2001).

58    N. H. Nahler, R. Baumfalk, U. Buck, Z. Bihary, R. B. Gerber, and B. Friedrich, *J. Chem. Phys.* **119**, 224 (2003).

59    N. H. Nahler, M. Fárník, and U. Buck, *Chem. Phys.* **301**, 173 (2004).

60    V. Poterya, O. Votava, M. Fárník, M. Ončák, P. Slavíček, U. Buck, and B. Friedrich, *J. Chem. Phys.* **128**, 104313 (2008).

61    M. Pettersson, L. Khriachtchev, A. Lignell, M. Räsänen, Z. Bihary, and R. B. Gerber, *J. Chem. Phys.* **116**, 2508 (2002).

62    V. I. Feldman and F. F. Sukhov, *Chem. Phys. Lett.* **255**, 425 (1996).

63    J. Lundell, S. Berski, and Z. Latajka, *Chem. Phys. Lett.* **371**, 295 (2003).

64    L. Sheng and R. B. Gerber, *J. Chem. Phys.* **126**, 021108 (2007).

65    V. E. Bondybey and G. C. Pimentel, *J. Chem. Phys.* **56**, 3832 (1972).

66    D. E. Milligan and M. E. Jacox, *J. Mol. Spectrosc.* **46**, 460 (1973).

67    C. A. Wight, B. S. Ault, and L. Andrews, *J. Chem. Phys.* **65**, 1244 (1976).

68    L. J. van IJzendoorn, L. J. Allamandola, F. Baas, and J. M. Greenberg, *J. Chem. Phys.* **78**, 7019 (1983).

69    H. Kunttu, J. Seetula, M. Räsänen, and V. A. Apkarian, *J. Chem. Phys.* **96**, 5630 (1992).

70    H. Kunttu and J. Seetula, *Chem. Phys.* **189**, 273 (1994).

71    M. Beyer, A. Lammers, E. V. Savchenko, G. Niedner-Schatteburg, and V. E. Bondybey, *Phys. Chem. Chem. Phys.* **1**, 2213 (1999).

72    M. Beyer, *Ph.D. Thesis*, Technische Universität München (1999).

73    V. A. Apkarian and N. Schwentner, *Chem. Rev. (Washington D.C.)* **99**, 1481 (1999).

74    G. Zundel and H. Metzger, *Z. Physik. Chem. (N.F.)* **58**, 225 (1968).

75    G. Zundel, in *The Hydrogen Bond – Recent Developments in Theory and Experiments. II. Structure and Spectroscopy*, edited by P. Schuster, G. Zundel, and C. Sandorfy, North-Holland, Amsterdam (1976), pp. 683-766.

76    D. Marx, M. E. Tuckerman, J. Hutter, and M. Parrinello, *Nature (London)* **397**, 601 (1999).

77    M. Beyer, E. V. Savchenko, G. Niedner-Schatteburg, and V. E. Bondybey, *Low Temp. Phys.* **25**, 814 (1999).

78    M. Beyer, E. V. Savchenko, and V. E. Bondybey, *Low Temp. Phys.* **29**, 1045 (2003).

79    P. E. Noble and G. C. Pimentel, *J. Chem. Phys.* **49**, 3165 (1968).

80    D. E. Milligan and M. E. Jacox, *J. Chem. Phys.* **53**, 2034 (1970).

81    V. Bondybey, G. C. Pimentel, and P. E. Noble, *J. Chem. Phys.* **55**, 540 (1971).

82    D. E. Milligan and M. E. Jacox, *J. Chem. Phys.* **55**, 2550 (1975).

83    B. S. Ault and L. Andrews, *J. Chem. Phys.* **63**, 2466 (1975).

84    B. S. Ault, *Acc. Chem. Res.* **15**, 103 (1982).

85    R. M. Bozorth, *J. Am. Chem. Soc.* **45**, 2128 (1923).

86    N. N. Greenwood and A. Earnshaw, *Chemistry of the Elements 2$^{nd}$ ed.*, Elsevier Butterworth-Heinemann, Burlington (2005), Chapter 17.

87    J. Lundell, M. Pettersson, and M. Räsänen, *Phys. Chem. Chem. Phys.* **1**, 4151 (1999).

88    J. Almlöf, *Chem. Phys. Lett.* **17**, 49 (1972).

89    D. R. Lide (ed.), *Handbook of Chemistry and Physics 81$^{st}$ ed.*, CRC press LLC, Boca Raton (2000).

90    C. Christides, D. A. Neumann, K. Prassides, J. R. D. Copley, J. J. Rush, M. J. Rosseinsky, D. W. Murphy, and R. C. Haddon, Phys. Rev. B 46, 12088 (1992).

91    G. A. Samara, L. V. Hansen, R. A. Assink, B. Morosin, J. E. Schirber, and D. Loy, *Phys. Rev. B* **47**, 4756 (1993).

92    S. A. Dzuba, *Phys. Lett. A* **213**, 77 (1996).

93    R. Fasel, R. G. Agostino, P. Aebi, and L. Schlapbach, *Phys. Rev. B* **60**, 4517 (1999).

94    L. J. Lauhon and W. Ho, *Phys. Rev. B* **60**, R8525 (1999).

95    B. B. Karki, R. M. Wentzcovitch, S. de Gironcoli, and S. Baroni, *Phys. Rev. B* **62**, 14750 (2000).

96    C. Moller and M. S. Plesset, *Phys. Rev* . **46**, 618 (1934).

97    C. C. J. Roothan, Rev. Mod. Phys. **23**, 69 (1951).

98    G. B. Bacskay, *Chem. Phys.* **61**, 385 (1981).

99    P. Pulay, *J. Comp. Chem.* **3**, 556 (1982).

100   M. J. Frisch, G. W. Trucks, H. B. Schlegel, G. E. Scuseria, M. A. Robb, J. R. Cheeseman, J. A. Montgomery, Jr., T. Vreven, K. N. Kudin, J. C. Burant, J. M. Millam, S. S. Iyengar, J. Tomasi, V. Barone, B. Mennucci, M. Cossi, G. Scalmani, N. Rega, G. A. Petersson, H. Nakatsuji, M. Hada, M. Ehara, K. Toyota, R. Fukuda, J. Hasegawa, M. Ishida, T. Nakajima, Y. Honda, O. Kitao, H. Nakai, M. Klene, X. Li, J. E. Knox, H. P. Hratchian, J. B. Cross, C. Adamo, J. Jaramillo, R. Gomperts, R. E. Stratmann, O. Yazyev, A. J. Austin, R. Cammi, C. Pomelli, J. W. Ochterski, P. Y. Ayala, K. Morokuma, G. A. Voth, P. Salvador, J. J. Dannenberg, V. G. Zakrzewski, S. Dapprich, A. D. Daniels, M. C. Strain, O. Farkas, D. K. Malick, A. D. Rabuck, K. Raghavachari, J. B. Foresman, J. V.

Ortiz, Q. Cui, A. G. Baboul, S. Clifford, J. Cioslowski, B. B. Stefanov, G. Liu, A. Liashenko, P. Piskorz, I. Komaromi, R. L. Martin, D. J. Fox, T. Keith, M. A. Al-Laham, C. Y. Peng, A. Nanayakkara, M. Challacombe, P. M. W. Gill, B. Johnson, W. Chen, M. W. Wong, C. Gonzalez, and J. A. Pople, *Gaussian 03, Revision C.02*, Gaussian, Inc., Wallingford CT, 2004.

101     M. W. Schmidt, K. K. Baldridge, J. A. Boatz, S. T. Elbert, M. S. Gordon, J. H. Jensen, S. Koseki, N. Matsunaga, K. A. Nguyen, S. Su, T. L. Windus, M. Dupuis, and J. A. Montgomey Jr, *J. Comp. Chem.* **14**, 1347 (1993).

102     Basis sets were obtained from the Extensible Computational Chemistry Environment Basis Set Database, Version 02/02/06, as developed and distributed by the Molecular Science Computing Facility, Environmental and Molecular Sciences Laboratory which is part of the Pacific Northwest Laboratory, P.O. Box 999, Richland, Washington 99352, USA, and funded by the U.S. Department of Energy. The Pacific Northwest Laboratory is a multi-program laboratory operated by Battelle Memorial Institute for the U.S. Department of Energy under contract DE-AC06-76RLO 1830. Contact Karen Schuchardt for further information.

103     K. L. Schuchardt, B. T. Didier, T. Elsethanger, L. Sun, V. Gurumoorthi, J. Chase, J. Li, and T. L. Windus, *J. Chem. Inf. Model.* **47**, 1045 (2007).

104     D. E. Woon and T. H. Dunning Jr., *J. Chem. Phys.* **98**, 1358 (1993).

105     R. A. Kendall, T. H. Dunning Jr., and R. J. Harrison, *J. Chem. Phys.* **96**, 6796 (1992).

106     R. Krishnan, J. S. Binkley, R. Seeger, and J. A. Pople, *J. Chem. Phys.* **72**, 650 (1980).

107     J-P. Blaudeau, M. P. McGrath, L. A. Curtiss, and L. Radom, *J. Chem. Phys.* **107**, 5016 (1997).

108     T. Clark, J. Chandrasekhar, P. V. R. Schleyer, *J. Comp. Chem.* **4**, 294 (1983).

109     A. Nicklass, M. Dolg, H. Stoll, and H. Preuss, *J. Chem. Phys.* **102**, 8942 (1995).

110     K. A. Peterson, D. Figgen, E. Goll, H. Stoll, and M. Dolg, *J. Chem. Phys.* **119**, 11113 (2003).

111     L. A. LaJohn, P. A. Christiansen, R. B. Ross, T. Atashroo, and W. C. Ermler, *J. Chem. Phys.* **87**, 2812 (1987).

112      N. Runeberg and P. Pyykkö, *Int. J. Quantum Chem.* **66**, 1313 (1998).

113      R. S. Mulliken, *J. Chem. Phys.* **23**, 1833 (1955).

114      A. E. Reed, L. A. Curtiss, and F. Weinhold, *Chem. Rev.* **88**, 899 (1988).

115      S. F. Boys and F. Bernardi, *Mol. Phys.* **19**, 553 (1970).

116      M. Rigby, E. B. Smith, W. A. Wakeham, and G. C. Maitland, *The Forces Between Molecules*, Oxford University Press, Oxford (1986).

117      R. T. Pack, *Chem. Phys. Lett* **55**, 197 (1978).

118      G. Rotzoll, *Chem. Phys. Lett* **88**, 179 (1982).

119      K. Morokuma, *J. Chem. Phys.* **55**, 1236 (1971).

120      K. Kitaura and K. Morokuma, *Int. J. Quantum Chem.* **10**, 325 (1976).

121      Z. Latajka, *J. Mol. Struct.:THEOCHEM* **251**, 245 (1991).

122      J. Lundell, M. Räsänen, and Z. Latajka, *J. Phys. Chem.* **97**, 1152 (1993).

123      R. W. Gora, W. Bartkowiak, S. Roszak, and J. Leszczynski, *J. Chem. Phys.* **117**, 1031 (2002).

124      J. Lundell and M. Pettersson, *Phys. Chem. Chem. Phys* **1**, 1691 (1999).

125      J. Lundell, S. Berski, and Z. Latajka, *Phys. Chem. Chem. Phys.* **2**, 5521 (2000).

126      A. V. Nemukhin, B. L. Grigorenko, L. Khriachtchev, H. Tanskanen, M. Pettersson, and M. Räsänen, *J. Am. Chem. Soc.* **124**, 10706 (2002).

127      S. A. C. McDowell, *Phys. Chem. Chem. Phys.* **5**, 808 (2003).

128      S. A. C. McDowell, *J. Chem. Phys.* **122**, 204309 (2005).

129      S. A. C. McDowell, *J. Chem. Phys.* **120**, 3630 (2004).

130      S. A. C. McDowell, *J. Chem. Phys.* **121**, 5728 (2004).

131      S. A. C. McDowell and A. D. Buckingham, *Spectroc. Acta. A* **61**, 1603 (2005).

132      S. A. C. McDowell, *Chem. Phys. Lett* **368**, 649 (2003).

133      S. A. C. McDowell, *J. Chem. Phys.* **118**, 4066 (2003).

134      S. A. C. McDowell, *J. Mol. Struct.:THEOCHEM* **625**, 243 (2003).

135      S. A. C. McDowell, *J. Chem. Phys.* **118**, 7283 (2003).

136      S. A. C. McDowell, *J. Chem. Phys.* **119**, 3711 (2003).

137      S. A. C. McDowell, *Chem. Phys. Lett.* **377**, 143 (2003).

138      S. A. C. McDowell, *Mol. Phys.* **101**, 2261 (2003).

139      S. A. C. McDowell, *Mol. Phys.* **102**, 71 (2004).

140      S. A. C. McDowell, *J. Mol. Struct.:THEOCHEM* **674**, 227 (2004).

141    S. A. C. McDowell, *Chem. Phys.* **301**, 53 (2004).

142    S. A. C. McDowell, *Mol. Phys.* **102**, 1441 (2004).

143    S. A. C. McDowell, *J. Mol. Struct.:THEOCHEM* **715**, 73 (2005).

144    S. A. C. McDowell, *Chem. Phys. Lett.* **406**, 228 (2005).

145    S. A. C. McDowell, *J. Mol. Struct.:THEOCHEM* **770**, 119 (2006).

146    S. A. C. McDowell, *Chem. Phys.* **328**, 69 (2006).

147    S. A. C. McDowell, *J. Comp. Chem.* **29**, 298 (2007).

148    S. A. C. McDowell and A. D. Buckingham, *Theor. Chem. Account* **119**, 29 (2008).

149    I. V. Alabugin, M. Manoharan, and F. A. Weinhold, *J. Phys. Chem. A* **108**, 4720 (2004).

150    J. Lundell, S. Berski, A. Lignell, and Z. Latajka, *J. Mol. Struct.* **790**, 31 (2006).

151    Y. Liu, W-Q. Liu, H-Y. Li, Y. Yang, and S. Cheng, *Chin. J. Chem. Phys.* **20**, 37 (2007).

152    S-Y. Yen, C-H. Mou, and W-P. Hu, *Chem. Phys. Lett.* **383**, 606 (2004).

153    M. Solimannejad and A. Boutalib, *Chem. Phys. Lett.* **389**, 359 (2004).

154    M. Sollimannejad, L. M. Amlashi, I. Alkorta, and J. Elguero, *Chem. Phys. Lett.* **422**, 226 (2006).

155    M. Solimannejad and I. Alkorta, *Chem. Phys.* **324**, 459 (2006).

156    M. Solimannejad and A. Boutalib, *Chem. Phys.* **320**, (2006).

157    M. Solimannejad and I. Alkorta, *Chem. Phys. Lett.* **439**, 284 (2007).

158    H. Tanskanen, S. Johansson, A. Lignell, L. Khriachtchev, and M. Räsänen, *J. Chem. Phys.* **127**, 154313 (2007).

159    J. W. C. Johns, *J. Mol. Spectrosc.* **106**, 124 (1984).

160    C. J. H. Schutte, *Chem. Phys. Lett.* **353**, 389 (2002).

161    I. Last and T. F. George, *J. Chem. Phys.* **89**, 3071 (1988).

162    M. T. Bowers and W. H. Flygare, *J. Chem. Phys.* **44**, 1389 (1966).

163    J. M. P. J. Verstegen, H.Goldring, S. Kimel, and B. Katz, *J. Chem. Phys.* **44**, 3216 (1966).

164    L. F. Keyser and G. W. Robinson, *J. Chem. Phys.* **44**, 3225 (1966).

165    D. E. Mann, N. Acquista, and D. White, *J. Chem. Phys.* **44**, 4353 (1966).

166    M. T. Bowers, G. I. Kerley, and W. H. Flygare, *J. Chem. Phys.* **45**, 3399 (1966).

167     M. G. Mason, W. G. Von Holle, and D. W. Robinson, *J. Chem. Phys.* **54**, 3491 (1970).

168     L. Andrews, B. J. Kelsall, and R. T. Arlinghaus, *J. Chem. Phys.* **79**, 2488 (1983).

169     A. Engdahl and B. Nelander, *J. Mol. Struct.* **193**, 101 (1989).

170     L. Khriachtchev, M. Pettersson, S. Jolkkonen, S. Pehkonen, and M Räsänen, *J. Chem. Phys.* **112**, 101 (2000).

171     K. Liu, A. Kolesov, J. W. Partin, I. Bezel, and C. Wittig, *Chem. Phys. Lett* **299**, 374 (1999).

172     M. Lorenz, D. Kraus, M. Räsänen, and V. E. Bondybey, *J. Chem. Phys.* **112**, 2803 (2000).

173     H. Tanskanen, L. Khriachtchev, J. Lundell, and M. Räsänen, *J. Chem. Phys.* **125**, 074501 (2005).

174     M. Pettersson, J. Lundell, L. Khriachtchev, and M. Räsänen, *J. Chem. Phys.* **109**, 618 (1998).

175     M. Pettersson, J. Lundell, L. Khriachtchev, E. Isoniemi, and M. Räsänen, *J. Am. Chem. Soc.* **120**, 7979 (1998).

176     S. Jolkkonen, M. Pettersson, and J. Lundell, *J. Chem. Phys.* **119**, (2003).

177     Z. Bihary, G. M. Chaban, and R. B. Gerber, *J. Chem. Phys.* **116**, 5521 (2002).

178     A. V. Bochenkova, D. A. Firsov, and A. V. Nemukhin, *Chem. Phys. Lett.* **405**, 165 (2005).

179     H. Flygare, *J. Chem. Phys.* **39**, 2263 (1963).

180     V. A. Apkarian and E. Weitz, *J. Chem. Phys.* **76**, 5796 (1982).

181     E. M. S. Maçôas, L. Khriachtchev, M. Pettersson, J. Juselius, R. Fausto, and M. Räsänen, *J. Chem. Phys.* **119**, 11765 (2003).

182     L. Khriachtchev, H. Tanskanen, M. Pettersson, M. Räsänen, V. Feldman, F. Sukhov, A. Orlov, and A. V. Shestakov, *J. Chem. Phys.* **116**, 5708 (2002).

183     L. Khriachtchev, M. Saarelainen, M. Pettersson, and M. Räsänen, *J. Chem. Phys.* **118**, 6403 (2003).

184     H. Tanskanen, L. Khriachtchev, A. Lignell, M. Räsänen, S. Johansson, I. Khyzhniy, and E. Savchenko, *Phys. Chem. Chem. Phys.* **10**, 692 (2008).

185     J. Nieminen and E. Kauppi, *Chem. Phys. Lett* **217**, 31 (1994).

186     J. R. Miller, *Science* **189**, 221 (1975).

187     J. Kron and C. Stradovski, *Int. J. Radiat. Phys. Chem.* **7**, 23 (1975).

188     K. I. Zamaraev, R. F. Khairutdinov, and J. R. Miller, *Chem. Phys. Lett.* **57**, 311 (1978).

189     L. E. Brus and V. E. Bondybey, *J. Chem. Phys.* **63**, 3123 (1975).

190     P. A. M. Dirac, *Proc. Roy. Soc.* **114**, 234 (1927).

191     E. Fermi, *Nuclear Physics*, The University of Chicago Press, Chicago (1950).

192     B. R. Henry M. Kasha, *Annu. Rev. Phys. Chem.* **19**, 161 (1968).

193     M. Razavy, *Quantum Theory of Tunneling*, World Scientific Publishing, Singapore (2003).

194     L. Khriachtchev, A. Lignell, H. Tanskanen, J. Lundell, H. Kiljunen, and M. Räsänen, *J. Phys. Chem.* **110**, 11876 (2006).

195     R. Kołos, M. Gronowski, and P. Botschwina, *J. Chem. Phys.* **128**, 154305 (2008).

196     T. R. Tuttle Jr. and S. Golden, *J. Phys. Chem.* **95**, 5725 (1991).

197     H. Abramczyk and J. Kroh, *J. Phys. Chem.* **95**, 5749 (1991).

198     H. Abramczyk and J. Kroh, *J. Phys. Chem.* **95**, 6155 (1991).

199     W. A. Caldwell, J. H. Nguyen, B. G. Pfrommer, F. Mauri, S. G. Louie, and R. Jeanloz, *Science* **227**, 930 (1997).

200     C. Sanloup, B. C. Schmidt, E. M. C. Perez, A. Jambon, E. Gregoryanz, and M. Mezouar, *Science* **310**, 1174 (2005).